

AN ABSTRACT OF THE CAPSTONE REPORT OF

Joo Hyung Park for the degree of Master of Chemical Sciences

Title: *4-Hydroxy-2-nonenal (HNE) Modification of Histidine 50 Affects the Biophysical Properties of α -Synuclein: Implications for Parkinson's Disease*

Project conducted at: Department of Chemistry
University of Pennsylvania, 231 S. 34 Street, Philadelphia, PA 19104
Supervisor: E. James Petersson

Dates of Project: May 2019-December 2020

Abstract Approved:

Parkinson's disease (PD) is a neurodegenerative disease that actively furthers the degeneration of dopaminergic neurons in substantia nigra and is characterized by the accumulation of α -synuclein (α S) in Lewy Bodies. During oxidative stress, increased levels of free radicals induce lipid peroxidation of polyunsaturated fatty acids, leading to the generation of reactive aldehydes within the body. Specifically, 4-hydroxy-2-nonenal (HNE) is known to be a lipid peroxidation product that can post-translationally modify α S, especially histidine 50 (H50). While studies have focused on the toxic effects of HNE-modified α S oligomers, no studies have determined how the site-specific H50-HNE interaction affects the biological and physical properties of α S. The purpose of this study is to identify how the site-specific modification of H50-HNE contributes to the pathogenesis of α S. To accomplish this, α S monomers were reacted with HNE, and the site-specific modification of H50 by HNE was confirmed using trypsin digest. These adducts were used to study its effect on α S aggregation, lipid binding, and cell uptake. Congo Red assay, incorporation assay, and dynamic light scattering (DLS) experiments showed that the H50-HNE modification was enough to significantly hinder the aggregation of α S, leading to a slower aggregation kinetics and smaller aggregate sizes. Moreover, the H50-HNE modification of α S induced a two-fold increase in lipid binding affinity, which may play a significant role in neurotransmitter release or synaptic vesicle integrity. Lastly, although both α S WT and HNE-modified monomers showed low levels of uptake in SH-SY5Y cells, where they were internalized by the lysosomal/endosomal system, the accuracy of these results is inconclusive and needs to be addressed in future studies. The data collectively demonstrate that H50-HNE modification alone can significantly affect the biophysical properties of α S.

4-Hydroxy-2-nonenal (HNE) Modification of Histidine 50
Affects the Biophysical Properties of α -Synuclein:
Implications for Parkinson's Disease

By

Joo Hyung Park

A CAPSTONE REPORT

Submitted to the University of Pennsylvania

In partial fulfillment of the requirements for the degree of
Master of Chemical Sciences

Presented on December 10, 2020
Commencement on December 20, 2020

Master of Chemical Sciences Capstone Report of

Joo Hyung Park

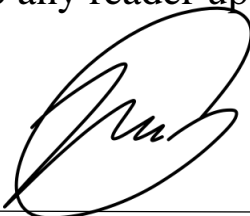
Presented on December 10, 2020

APPROVED:



E. James Petersson, Representing Biological Chemistry

I understand that my Capstone Report will become part of the permanent collection of the University of Pennsylvania Master of Chemical Sciences Program. My signature below authorizes release of my final report to any reader upon request



Joo Hyung Park, Author

Acknowledgements

First, I would like to thank my lab members for helping me adjust to the lab and helping me become a better scientist. They have been incredible people who demonstrated the necessary knowledge and commitment to pursue lab work. It was due to their work ethic, teamwork, and communication that highly motivated me to become a better scientist for the lab. I would particularly like to express gratitude to my mentor, Buyan Pan, for investing considerable time to teach me the basic skills needed for my research project. Her dedication to help her mentees and offer important advices has been a key reason for the progress of this project. Also, she exemplified great tolerance and patience for some of my inexperience and novice mistakes. None of this would have been possible without her help. Second, I would like to thank my project advisors, Dr. E. James Petersson and Dr. Elizabeth Rhoades, for guiding me through this project. Even though I was a new master's student, they allowed me to actively participate in various activities such as research group meetings and journal club. These activities really helped me develop my presentation and communications skills, which are important in becoming a well-rounded scientist. They also graciously offered resources for my new project and gave valuable feedback regarding my project. In many ways, I could not have asked for better advisors. Third, I would like to thank Dr. Ana-Rita Mayol for guiding me through academically. Due to COVID-19, there were many challenges that I faced but she helped me navigate through those obstacles. Fourth, I would like to thank the chemistry department and staff members for allowing me to pursue my master's degree without major issues. Lastly, I would like to express my appreciation and love for my family who unconditionally supported me throughout my life and career.

Table of Contents

Abstract	i
Title Page	ii
Approval Page	iii
Acknowledgments	iv
Table of Contents	v
List of Figures	vi
List of Appendices	vii
Introduction.....	1
Materials and Methods.....	7
Results and Discussion	13
Conclusion	29
Reference	30
Appendices.....	33

List of Figures

Figure 1. The Pathogenesis of Parkinson’s disease	2
Figure 2. Pathway of HNE Formation and Reactivity towards Histidine and Lysine.	3
Figure 3. Synthesis of HNE-modified α -synuclein monomers labeled with Atto488.	5
Figure 4. Different Concentrations of HNE reacted with α -synuclein at 37 °C overnight	14
Figure 5. Separation of each HNE-modified α -synuclein.....	15
Figure 6. MALDI of Trypsin Digest peptides of H50-modified α -synuclein.....	16
Figure 7. MALDI masses of α S samples before starting aggregation experiment	18
Figure 8. Congo Red Aggregation Assay for α S WT and α S H ₅₀ -HNE	19
Figure 9. MALDI-MS showing the masses of the α S H ₅₀ -HNE sample at 60-hour timepoint	19
Figure 10. Quantification of α s incorporated in fibrils and aggregates with SDS-PAGE	20
Figure 11. DLS of α s WT fibrils and α s HNE-modified aggregates	22
Figure 12. Purification of α -synuclein PpY114	23
Figure 13. HNE-modification to α -synuclein PpY114	23
Figure 14. HPLC Purification of H50 HNE-modified α -Synuclein PpY114	24
Figure 15. Labeling HNE-modified α -synuclein PpY114 with Atto488-azide	25
Figure 16. The binding affinity curves of α S WT and α S-H50-HNE samples on lipid vesicles.....	27
Figure 17. Cell uptake and internalization experiments of α S WT and α S-H50-HNE samples with SH-SY5Y cells.....	28

List of Appendices

Appendix 1. SDS-PAGE gel of incorporated α S in aggregated samples of α S WT and α S-H50-HNE	33
Appendix 2. Autocorrelation curves for α S-H50-HNE samples in buffer, 0.01 mM POPS/PC, and 0.01 mM POPS/PC.....	34

Introduction

Parkinson's disease (PD) is a neurodegenerative disorder that promotes progressive loss of dopaminergic neurons in the substantia nigra and accumulates abnormal aggregates of protein called "Lewy Bodies".^{1,2} It is the second most common neurodegenerative disease and contributes to tremor, bradykinesia, rigidity, postural instability, neuropsychiatric disturbances, and sleep disorders. Many risk factors have been proposed, but it is believed that α -synuclein (α S) plays an important role in its pathology.^{1,2}

α S is an intrinsically disordered protein (IDP), a protein that lacks a definitive secondary or tertiary structure. It consists of three distinct domains: the N-terminus (residues 1-60), with KTEGV motif repeats; the hydrophobic domain (residues 61-95), also called the non-amyloid component (NAC); and the C-terminus (residues 96-140), enriched with acidic amino acids.^{3,4} IDPs such as α S can play important roles in modulating and regulating biological systems due to their structural plasticity, flexible binding capability, and environmental sensitivity. The main function of α S has remained unclear, despite intense research in the field. However, due to its localization in pre-synaptic terminals and interaction with synaptic components, it is suggested that α S is likely associated with the function of synapse, such as neurotransmitter release, dopamine metabolism, vesicle trafficking, and other important activities.⁵⁻¹⁰ Other functions, such as molecular chaperoning, DNA repair, and antioxidant activity, have been proposed as well.¹¹⁻¹³ Although α S is highly localized in pre-synaptic terminals, it is also found in red blood cells, body tissues, and organs.¹⁴

Under certain stressed conditions, α S monomers can undergo misfolding and aggregate into oligomers and protofilaments enriched in β -sheet content (**Figure 1**). Protofilaments can form longer, bundled fibrils that are toxic to the brain. Since misfolded proteins can induce other monomers to misfold and aggregate, these toxic fibrils tend to accumulate in Lewy bodies and are believed to be the cause of neuronal death (**Figure 1**).^{1,2,7,15} Therefore, it is believed that α S contributes to the neurotoxicity found in PD, meaning that the investigation in the biophysical properties of α S may shed light on finding possible therapeutic options for PD and other related neurodegenerative diseases.

In recent years, it has been proposed that α S function and pathology can be altered by post-translational modifications (PTMs). Many PTMs such as phosphorylation, acetylation, ubiquitination, truncation, and nitration have been studied, and their effects on vesicle binding, conformational properties, and cell toxicity have been characterized.¹⁶ The most prototypical PTM is phosphorylation of serine 129 (pS129), where a significant increase of pS129 was observed within LBs, suggesting a role in its pathology and aggregation.¹⁷⁻¹⁹ Another important PTM is aldehyde-induced covalent modification. It was first suggested that lipid peroxidation of polyunsaturated fatty acids (PUFA) generates toxic aldehyde species, most notably 4-hydroxy-2-nonenal (HNE) (**Figure 2A**).²⁰ During oxidative stress, the oxygen-derived free radicals induce lipid peroxidation and interact with PUFA to produce toxic aldehyde species (**Figure 2**). However, recent studies have shown that lipid peroxidation is not the only source of HNE production in

the body. Food consumption has also been implicated to be a source of HNE accumulation within the body, especially those cooked with oxidized oil (**Figure 2A**).²¹ Nonetheless, HNE can react with proteins and form adducts, most notably a Michael Addition reaction with histidine or Schiff Base reaction with lysine (**Figure 2B**).²⁰

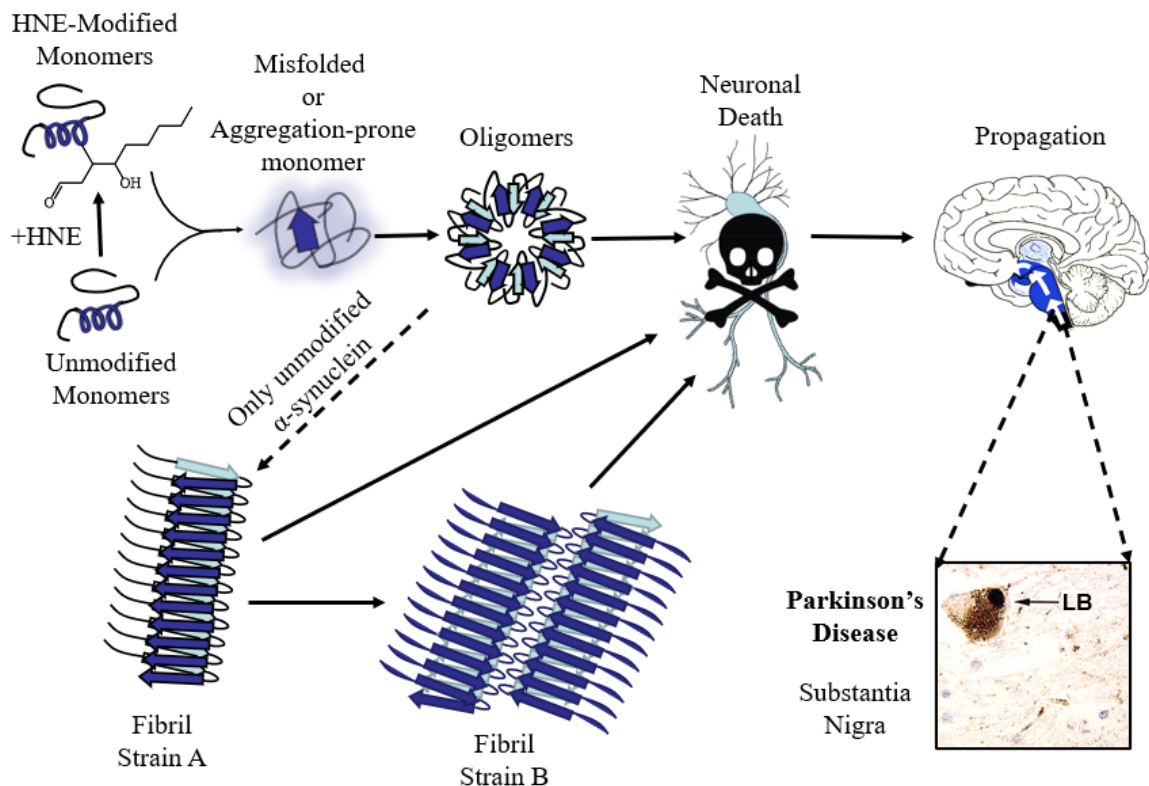


Figure 1. The Pathogenesis of Parkinson's disease. Aggregation-prone α S monomers aggregate to form oligomers. Oligomers from unmodified α S can form fibrils, while HNE-modified α S do not develop in fibrils. Regardless, both lead to neuronal death and cell toxicity. If oligomers and fibrils accumulate in the brain, it leads to toxic Lewy bodies within substantia nigra.^{1, 2, 15, 22}

While HNE can accumulate in tissues and organs throughout the body, the central nervous system is highly vulnerable to such aldehydes due to its high levels of polyunsaturated lipids in neuronal cell membranes and poor antioxidative defenses. It is believed that lipid peroxidation products increase with ageing.²⁰ Therefore, age-related diseases such as neurodegenerative diseases, obesity, and metabolic syndrome have been implicated to be affected by HNE and other lipid peroxidation products.²³ In neurodegenerative diseases, many studies have shown increased oxidation of the brain lipids, carbohydrates, proteins, and DNA. In Alzheimer's disease, HNE is found to impair glucose transport in rat hippocampal neurons, block glutamate transport in rat neocortical synaptosomes, cause neuronal death and cell apoptosis, and inhibit degradation mechanism of oxidized proteins by the proteasome.^{24, 25} In PD, HNE-protein adducts were found in Lewy Bodies and in mitochondria in PD and other Lewy Body diseases.^{26, 27} Many studies have explored the effects of HNE-induced modifications on

α S. In the study by Qin, HNE induced the formation of α S oligomers and promoted increased β -sheet formation, inhibited fibril formation, and increased neurotoxicity (**Figure 1**).²² Xiang discovered that HNE preferentially interacted with histidine 50 before reacting with other lysine residues, possibly indicating an important role of H50 in α S pathology.²⁸

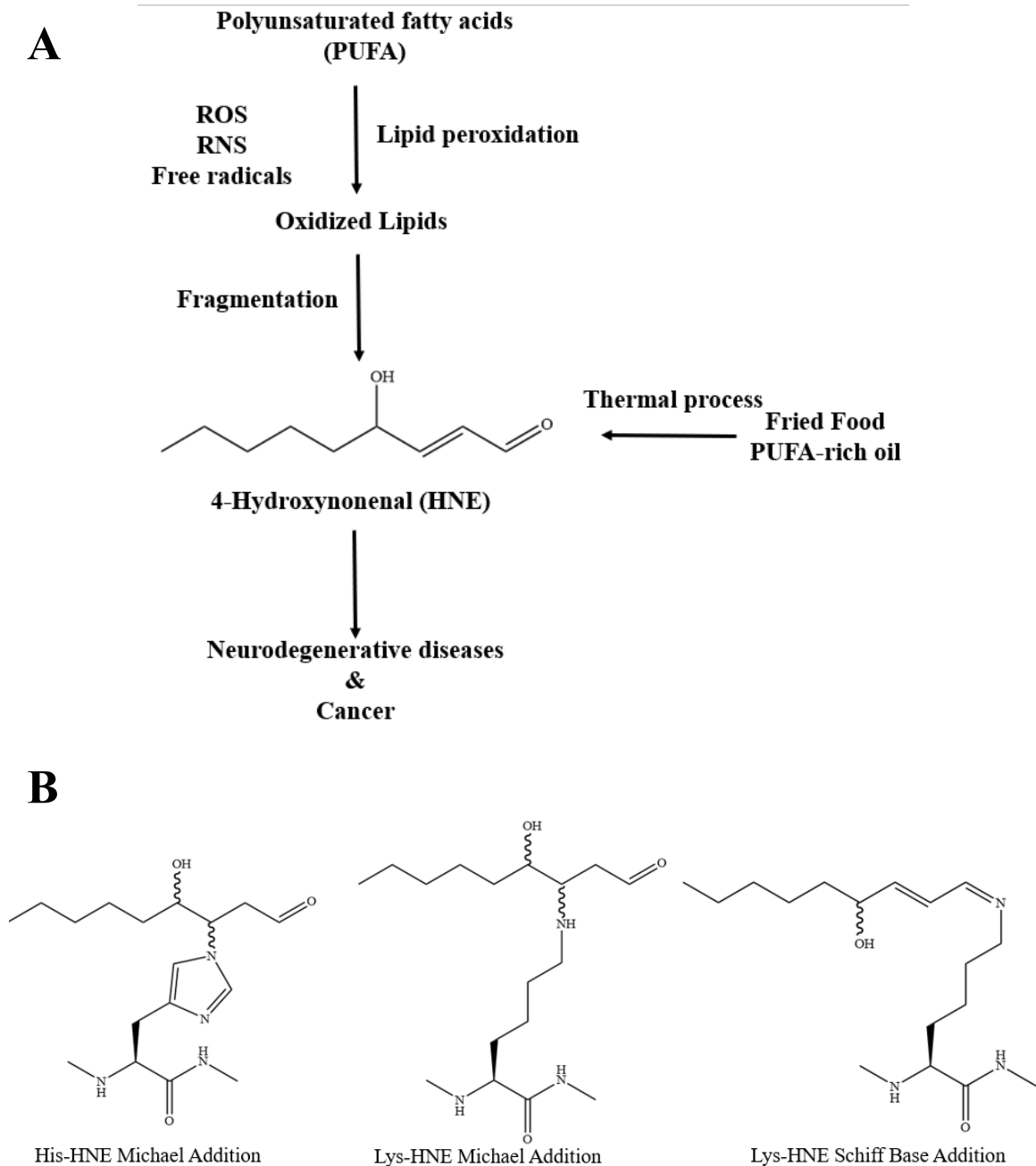


Figure 2. Pathway of HNE Formation and Reactivity towards Histidine and Lysine.

The recent utilization of cryo-electron microscopy (cryo-EM) to elucidate the fibril structures of α S shed light on the importance of residue H50 in its fibril formation. It was found that fibril structure was stabilized through the salt-bridge interaction of E57 and H50 of two protofilaments, meaning that the fibril structure is highly influenced by changes to the H50.²⁹ These findings were further supported by Boyer when their cryo-EM structure of H50Q α S fibrils showed previously unobserved polymorphs, demonstrating how modifications to the H50 residue can influence aggregate structure and thus cytotoxicity of α S.³⁰ These studies have implied that H50 may have a positional significance in fibril formation and produce different effects on its biophysical properties, depending on the nature of the modification. This raises a natural question of whether HNE-induced α S pathogenesis is caused by the site-specific alteration at H50 by HNE. While many studies have focused on HNE-induced α S oligomers, no studies have explored the specific effects of H50-HNE modification on α S monomers (α S-H50-HNE).

The goal of this project is to study the biochemical consequence of having α S H50 modified by HNE, especially the implications for its pathology. To accomplish this goal, the project was divided into four important objectives: 1) observe how HNE reacts with α S, 2) monitor how HNE modification on H50 affects α S aggregation properties, 3) measure the effects of HNE-H50 interaction on lipid binding, and 4) investigate how this site-specific interaction affects cell uptake and internalization.

The first part of this project will consist of *HNE reaction with α S*. HNE will be directly reacted with α S and purified using high performance liquid chromatography (HPLC). Taking advantage of HNE electrophilic reactivity and the nucleophilic nature of H50, it is likely that HNE will preferentially react with H50 before any other lysine residues. Thus, the purified single Michael addition adducts will likely represent the H50-HNE modification. To verify that H50 is the first residue to react with HNE, the purified Michael addition adducts were analyzed through trypsin digest. Matrix-assisted laser desorption/ionization (MALDI-MS) will be used to monitor the mass changes that correlate with the HNE modification on α S.

Characterization of α S Aggregation will be the second part of the project. Congo red assay, SDS-PAGE, and dynamic light scattering (DLS) were used to characterize the effects of H50-HNE modification on α S aggregation. Congo Red is a dye that has a high affinity towards amyloid structures and will be used in an assay to measure the kinetics of α S aggregation. To help characterize the size of α S aggregates and the degree of α S incorporation, dynamic light scattering (DLS) and SDS-PAGE analysis will be used, respectively. Due to past studies showing the involvement of H50 in fibril formation²⁸, it was hypothesized that the specific interaction of H50 and HNE will alter how α S normally aggregates over time.

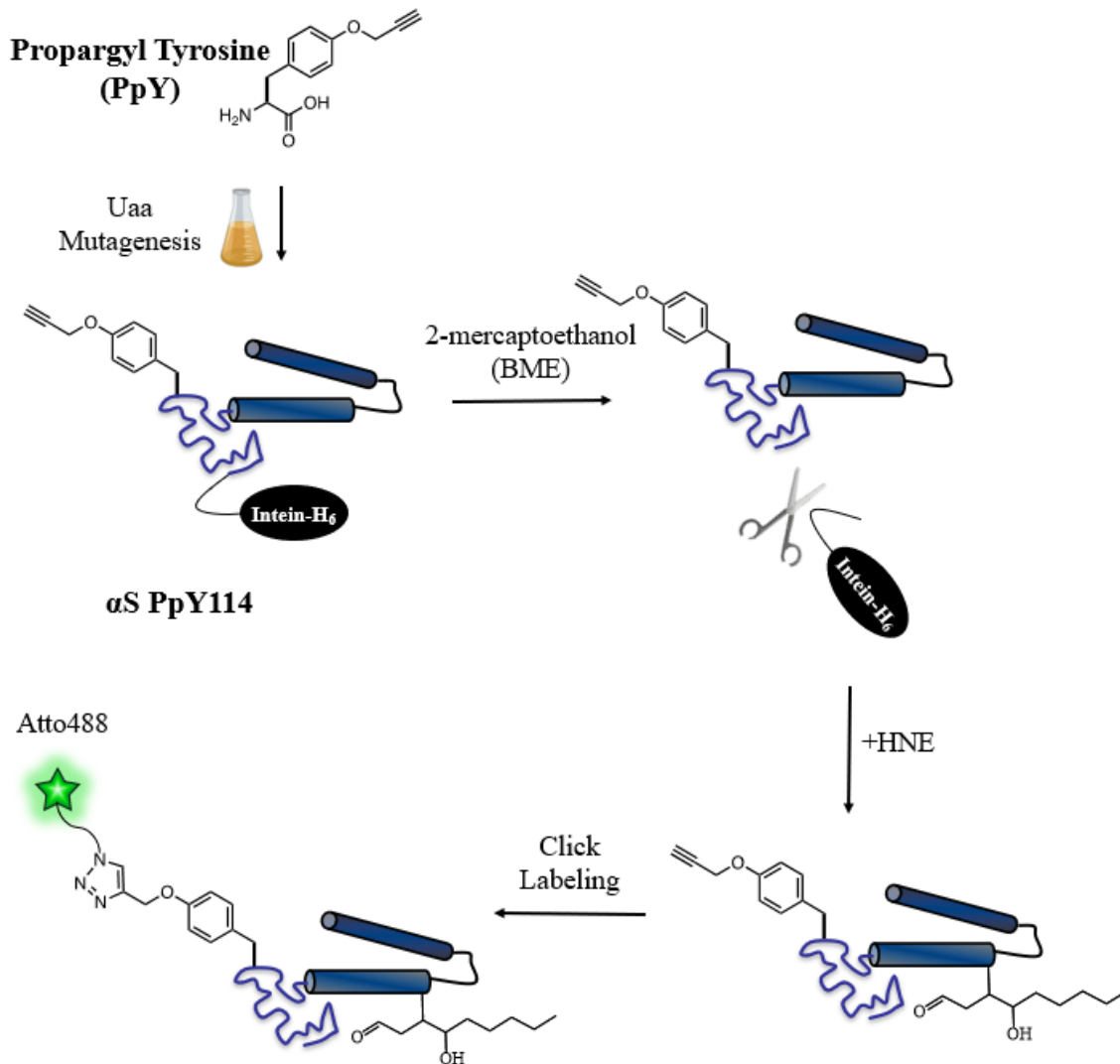


Figure 3. Synthesis of HNE-modified α -synuclein monomers labeled with Atto488. Unnatural amino acid mutagenesis was achieved to express α -synuclein PpY114. Click chemistry can be used to label α -synuclein at position 114 where propargyl tyrosine (PpY) was incorporated through unnatural amino acid mutagenesis.

The third part of the experiment is the *Measurement of α S lipid binding*. The HNE-modified α S were fluorescently labeled, and lipid binding was observed using fluorescence correlation spectroscopy (FCS). Because FCS measures the dependence of fluorescence intensity fluctuations on particle size, a fluorescent probe was designed to label α S without perturbing its native aggregating or lipid binding properties. Cysteine-maleimide labeling cannot be utilized for this experiment since the thiol group of cysteine is highly nucleophilic and will more favorably react with HNE over H50 during the modification process. Instead, unnatural amino acid (Uaa) mutagenesis will be used to incorporate an alkyne biorthogonal reactive handle that will specifically interact with fluorescent molecule (**Figure 3**). By utilizing Uaa mutagenesis, α S is expressed with propargyl tyrosine (PpY) incorporated at position 114, a position that is not involved in α S lipid binding or aggregation. PpY 114 later will undergo alkyne-azide click chemistry

to attach Atto488 (**Figure 3**). Thus, these fluorescently-labeled α S will be introduced to lipid vesicles, and lipid binding will be monitored using FCS.

The project will be culminated with *Cell uptake and internalization studies*. The fluorescently labeled α S with H50-HNE modification will be introduced to SH-SY5Y cells to analyze cell uptake and localization data. Fluorescence microscopy is used to qualitatively analyze cell uptake and internalization of fluorescently labeled α S within the cells. To determine α S internalization within the cells, lysosomal biomarker will be added as well.

Materials and Methods

General Considerations

Bioreagents, Chemicals, and Materials

Ampicillin, CaCl₂, Tris buffer, ZnCl₂, and CuSO₄ were purchased from Fisher. Streptomycin was purchased from MP Biomedicals. HEPES buffer, FeCl₂, MgSO₄, THPTA, sodium ascorbate, and Atto488-azide were purchased from Sigma-Aldrich. isopropyl- β -D-1-thiogalactopyranoside was purchased from Lab Scientific. HiTrap™ Q HP column was purchased from GE Healthcare. 2-mercaptoethanol was purchased from BioRad. Imadazole was purchased from Alfa Aesar. Ni-NTA resin was purchased from GoldBio. Lysotracker Deep Red was purchased from Life Technologies (Carlsbad, CA). HNE was purchased from Cayman Chemical.

Instruments

MALDI-MS was performed using Bruker Ultraflex III. Protein purification was achieved by using FPLC (Amersham AKTA Explorer FPLC). Modification adducts were purified using Varian Prostar system (Agilent Technologies; Santa Clara, CA) HPLC on a C4 column (Grace Davison Discovery Sciences). Congo Red absorbance was measured using Tecan Infinite M1000 plate reader (Mannedorf, Switzerland). Protein aggregate sizes were analyzed using Malvern Zetasizer Nano. Olympus IX71 microscope (Spectra-Physics) was used to develop a lab-built instrument capable of FCS measurements.

HNE reaction with α S

Expression of wildtype α S and α S with unnatural amino acid PpY incorporated at position 114

To express α S WT, the plasmid containing the α S gene fused with an intein and His purification tag was transformed into *E. coli* BL21 cells.^{31,32} This was accomplished by mixing the BL21 cells with the plasmid for 15 minutes on ice and heat shocking the sample at 42 °C for 30 seconds. Afterwards, the sample was rested on ice for 2 minutes before 950 μ L of Super Optimal broth with Catabolite repression (SOC) media was added. Then, the sample was incubated in 37 °C for one hour. The sample was plated on LB/ampicillin (Fisher Bioreagents) plate (100 μ g/mL of antibiotics) and incubated overnight.

After colonies were observed, the colonies were transferred to 5 mL of LB media supplemented with 100 μ g/mL of ampicillin for α S WT. The primary cultures were incubated at 37 °C while shaking at 250 rpm. After growing the primary cultures, they were transferred into 1 mL of LB media. After inoculation, the bacterial samples were grown at 37 °C while shaking at 250 rpm. When OD₆₀₀ reached 0.7-1.0, isopropyl- β -D-1-thiogalactopyranoside (IPTG, Lab Scientific) was added to a final concentration of 1 mM. The cultures were incubated at 18 °C overnight while shaking at 250 rpm.

After overnight induction, the samples were spun at 4,000 rpm for 30 minutes. The supernatant was removed, and the cell pellets were mixed with resuspension buffer (40 mM Tris buffer, pH 8.3 with 1 Roche protease inhibitor cocktail pill). The resuspended cell samples were sonicated on ice (sonication: amplitude 30, 5 minutes, 1 second on, 1 second off) and the cell debris was centrifuged (14,00 rpm, 20 minutes, 4 °C).

The supernatant was purified by incubating it with 3 mL of Ni-NTA resin (GoldBio). The supernatant with Ni-NTA resin was washed with 15 mL of 50 mM HEPES buffer (pH 7.5; Sigma Aldrich) and 20 mL of 5 mM HEPES buffer with 200 mM imidazole (Alfa Aesar) at pH 7.5. The protein was eluted with 12 mL of 50 mM HEPES buffer with 300 mM imidazole (pH 7.5). 2-mercaptoethanol (BME, BioRad) was added to the eluted protein sample to 200 mM final concentration, and the solution allowed to react at room temperature overnight. Afterwards, the protein samples were dialyzed at 4 °C in 20 mM Tris (pH 8.0) overnight and underwent a reverse nickel column purification to remove the cleaved intein with the His₆ tag. MALDI-MS, an ionization technique based on mixing protein sample with laser energy absorbing matrix, was utilized to confirm the identity of the expressed protein. The masses were confirmed on MALDI-MS (Bruker Ultraflex III; Billerica, MA). The dialyzed samples underwent FPLC (Amersham AKTA Explorer FPLC) on a HiTrap™ Q HP column (GE Healthcare) to purify the desired α S products.

HNE modification of α S

To confirm that HNE can modify α -synuclein through Michael addition, different concentrations of HNE (Cayman Chemical) and WT α S were incubated together overnight in PBS (pH 7.4) at 37 °C. The modifications were confirmed using MALDI-MS.

Purification of singly-modified α S monomers

To purify the specific H50-modified α S, a mixture of α S and HNE (1:5-1:10 ratio) was incubated at 37 °C overnight. The samples were purified with the Varian Prostar system (Agilent Technologies; Santa Clara, CA) HPLC, where proteins with different levels of modification were separated and then the fractions were lyophilized.

Trypsin Digest Protocol

The lyophilized samples were mixed with 25 μ L of dissolving agent of 6 M Gdn-HCl (Invitrogen)+50 mM Tris (Fisher Scientific) at pH 8. Afterwards, 5 μ L of 10 mM BME was added to the reaction. The samples were heated at 95 °C for 5-10 minutes. After denaturation, the reaction was cooled for several minutes before diluting and spin filtering the samples with 50 mM Tris-HCL (pH 7.6; Fisher Scientific). After reducing the Gdn-HCl concentration below 1 M, the samples were mixed with 1.55 μ L of 1 mM CaCl₂ (Fisher Chemical). For protein digestion, 1 μ L of 1 mg/mL trypsin was added to samples, and these samples were incubated at 37 °C overnight. The peptide sizes were confirmed using MALDI-MS.

Characterization of α S Aggregation

Aggregation Assay

α S WT or α S H50-HNE samples (300 μ L of 100 μ M) in Tris buffer (20 mM Tris, 100 mM NaCl, pH 7.5) were incubated in 37 °C while shaking at 1300 rpm. Absorbance measurements at various time points (0, 4, 6, 8, 10, 12, 24, 28, 32, 36, 48, 60 hours) were taken by mixing 140 μ L of Congo Red (20 μ M in 20 mM Tris, 100 mM NaCl pH 7.5) with 10 μ L of sample. Tecan Infinite M1000 plate reader (Mannedorf, Switzerland) was used to measure the absorbance at 480 nm and 540 nm.

Dynamic Light Scattering (DLS)

Taking the samples from the aggregation samples, 160 μ L of were taken from each sample and diluted with 500 μ L Tris buffer (20 mM Tris, 100 mM NaCl, pH 7.5) in disposable cuvettes (BrandTech™ BRAND™ Plastic Cuvettes). Measurements were taken on the Malvern Zetasizer Nano (Dispersant RI: 1.332, Viscosity: 0.9020). The size of a particle was calculated by using the Stokes-Einstein equation:

$$d(H)=kT/(3\pi\eta D) \quad (1)$$

where $d(H)$ is the hydrodynamic diameter, D is translational diffusion coefficient, k is Boltzmann's constant, T =absolute temperature, and η is viscosity.

Quantification of total α S incorporation SDS-PAGE gel

After aggregating the α S WT and α S-HNE samples, 30 μ L of each were spun down at 13,200 rpm for 90 minutes at 4 °C. Afterwards, the supernatant was discarded, and the pellet was resuspended in 30 μ L Tris buffer (20 mM Tris, 100 mM NaCl, pH 7.5). 10 μ L of each sample was combined with SDS (final concentration at 25 mM). The combined samples were boiled on heat block for 20 minutes and cooled in ice for 10-15 minutes. 3 μ L of 4x loading dye and loaded onto the SDS-PAGE (18% acrylamide, Coomassie stain). Band intensity quantification was performed with NIH ImageJ software.

Measurement of α S lipid binding

Expression of α S with unnatural amino acid PpY incorporated at position 114

For α S PpY114 expression, the α S plasmid containing a TAG codon at position 114 (2-3 μ L) was added to 50 μ L of *E. coli* BL21 cells containing orthogonal tRNA_{CUA} and pXF-tRNA synthetase pair encoded by the pDULE-pXF plasmid.³² After allowing the mixture to rest on ice for 30 minutes, the sample was heat shocked at 42 °C for one minute and put onto ice for two minutes. SOC media (450 μ L) was added and the mixture was incubated at 37 °C for one hour. The sample was plated on LB/ampicillin (Fisher

Bioreagents)/streptomycin (MP Biomedicals) plates (100 µg/mL of each antibiotics) and incubated overnight.

Afterwards, the colonies were transferred to 5 mL of LB media supplemented with ampicillin/streptomycin. The primary cultures were incubated at 37 °C while shaking at 250 rpm. After growing the primary cultures, they were transferred into 500 mL of M9 media (500 mL M9 salts, 1 mL 10% w/v yeast extract (Millipore), 6.25 mL 40% w/v glucose, 500 µL of 15 mg/mL ZnCl₂ (Fisher Scientific), 500 µL of 15 mg/mL FeCl₂ (Sigma-Aldrich), 1 mL of 1 M MgSO₄ (Sigma-Aldrich), 0.5 µL of CaCl₂, 100mg/L ampicillin and streptomycin). After inoculation, the bacterial samples were grown at 37 °C while shaking at 250 rpm. When OD₆₀₀ reached 0.7-1.0, 110 mg of PpY (dissolved in MilliQ water) were added before isopropyl-β-D-1-thiogalactopyranoside (IPTG, Lab Scientific) was added to a final concentration of 1 mM. The cultures were incubated at 18 °C overnight while shaking at 250 rpm.

After overnight induction, the samples were spun at 4,000 rpm for 30 minutes. The supernatant was removed, and the cell pellets were mixed with resuspension buffer (40 mM Tris buffer, pH 8.3 with 1 Roche protease inhibitor cocktail pill). The resuspended cell samples were sonicated on ice (sonication: amplitude 30, 5 minutes, 1 second on, 1 second off) and the cell debris was centrifuged (14,00 rpm, 20 minutes, 4 °C).

The supernatant was purified by incubating it with 3 mL of Ni-NTA resin (GoldBio). The supernatant with Ni-NTA resin was washed with 15 mL of 50 mM HEPES buffer (pH 7.5; Sigma Aldrich) and 20 mL of 5 mM HEPES buffer with 200 mM imidazole (Alfa Aesar) at pH 7.5. The protein was eluted with 12 mL of 50 mM HEPES buffer with 300 mM imidazole (pH 7.5). 2-mercaptoethanol (BME, BioRad) was added to the eluted protein sample to 200 mM final concentration, and the solution allowed to react at room temperature overnight. Afterwards, the protein samples were dialyzed at 4 °C in 20 mM Tris (pH 8.0) overnight and underwent a reverse nickel column purification to remove the cleaved intein with the His₆ tag. MALDI-MS, an ionization technique based on mixing protein sample with laser energy absorbing matrix, was utilized to confirm the identity of the expressed protein. The masses were confirmed on MALDI-MS (Bruker Ultraflex III; Billerica, MA). The dialyzed samples underwent FPLC (Amersham AKTA Explorer FPLC) on a HiTrap™ Q HP column (GE Healthcare) to purify the desired α-synuclein products.

HNE-modification of αS PpY114

HNE (5-10 molar equivalents) was added to 1 molar equivalent of αS. The mixture was incubated overnight in PBS (pH 7.4) at 37 °C. To purify the H50-modified αS, the mixed sample were injected into Varian Prostar system (Agilent Technologies; Santa Clara, CA) HPLC, and the singly modified αS species were separated on a C4 column (Grace Davison Discovery Sciences). The identities of the samples were confirmed with MALDI-MS analysis.

Labeling of HNE-modified α S with Atto488

One molar equivalent of the protein sample was mixed with the catalytic mixture (2 molar equivalents of CuSO_4 (Fisher Scientific), 10 molar equivalents of THPTA (Sigma-Aldrich), 20 molar equivalents of sodium ascorbate (Sigma-Aldrich), 1.5 molar equivalent of dye-azide). Atto488-azide (Sigma-Aldrich) was used for labeling in this experiment. The mixture was incubated at 37 °C for 2 hours. After completion of the reaction was confirmed, TCEP was added to a final concentration of 30 mM and incubated at room temperature for 20 minutes. Then, the labeled sample was purified by Varian Prostar system (Agilent Technologies; Santa Clara, CA) HPLC, and purified fractions were lyophilized. The lyophilized products were stored in a vial at room temperature.

Using FCS to determine lipid binding

α S samples labeled with Atto488 were introduced with various lipid vesicle concentrations (0.005 mM-0.5 mM) consisting of 50:50; POPS/POPC. The autocorrelation curve was fit to a 2-component equation³³:

$$G(\tau)=1/N \times [(A \times 1/(1+\tau/\tau_1) \times (1/(1+s^2\tau/\tau_1))^{1/2})] + [Q \times (1-A) \times 1/(1+\tau/\tau_2) \times 1/(1+s^2\tau/\tau_2)^{1/2}] \quad (2)$$

where is $G(\tau)$ the autocorrelation function, N is the number of molecules in the focal volume, τ_1 is the characteristic diffusion time of α S, τ_2 is the characteristic diffusion time of the vesicles, s is a structural factor of the instrument, Q is the brightness factor, and A is the fraction of α S bound. To fit autocorrelation curves for α S in the presence of lipid vesicles, it was important to fix the diffusion time of bound and unbound α S with experimentally determined values. Diffusion time of the unbound α S, τ_1 was determined by measuring protein in buffer without lipids. The diffusion time of vesicles, τ_2 , was determined by measuring protein in presence of saturated concentration of vesicles (2 mM lipid). BODIPY-labeled 50:50 POPS/POPC, which are the same size of unlabeled vesicles, were used to confirm the diffusion time of the vesicles. For the binding assay, the fraction of α S bound at each concentration was obtained from fitting to each autocorrelation curve. Averages and standard deviations were calculated at each lipid concentration. The binding curve fit of the following equation³⁴ was used to determine $K_{d,app}$:

$$A = B_{max}x/(K_{d,app}+x) \quad (3)$$

where A is the fraction of α S bound, x is the accessible lipid concentration, B_{max} is the maximum fraction of α S bound, and $K_{d,app}$ is the apparent dissociation constant.

For FCS, eight-well chambered cover glasses (Nunc: Rochester, NY) underwent plasma cleaning before incubating it overnight with polylysine-conjugated polyethylene glycol (PEG-PLL; Pierce), which was prepared using a lab-built PEGylation protocol. Afterwards, the chambers were washed and stored in MilliQ water. A lab-built instrument derived from a Olympus IX71 microscope (continuous emission 488 nm DPSS 50 mW laser; Spectra-Physics, Santa Clara, CA) was used for FCS measurements. With the laser

power was set to 4.5 μ W, fluorescence emission that were collected from the objective was separated from the excitation signal with a Z488rdc long pass dichroic filter and an HQ600/200nm bandpass filter (Chroma, Bellows Falls, VT). The emission signal was focused onto the aperture of a 50 μ m optical fiber, and signal amplification was obtained by an avalanche photodiode (Perkin Elmer, Waltham, MA). A digital autocorrelator (Flex03Q-12, correlator.com, Bridgewater, NJ) was used to obtain autocorrelation curves (30 correlation curves of 30 seconds for each measurement), and fitting was accomplished with a lab-written code in MATLAB (The MathWorks, Natick, MA)

Cell uptake and internalization studies

Cell uptake and localization of α S in SH-SY5Y Cells

SH-SY5Y cells were grown at 37 °C in a humidified atmosphere of 5% CO₂. The cells were cultured in Dulbecco's Modified Eagle's Medium (DMEM) plus 10% fetal bovine serum, 50 U/ml penicillin, and 50 μ g/ml streptomycin. Cells were passaged upon reaching approximately 95% confluence (0.05% Trypsin-EDTA, Life Technologies, Carlsbad, CA) and propagated. For experimental use, the cells were pelleted and resuspended in fresh media that lack Trypsin-EDTA.

Cell imaging was performed with a confocal fluorescence microscopy (Olympus FV3000 scanning system assembled on a IX83 inverted microscope platform, 60 \times Plan-Apo/1.1-NA water-immersion objective with DIC capability; Tokyo, Japan). Since Atto488 was used for labeling, the gaining setting for the blue channel was used (excitation 488 nm, emission BP 500-540 nm). Images were obtained in 8-well ibidi chambers (μ -Slide, 8-well glass bottom, ibidi GmbH, Germany) coated with poly-D-lysine.

For cell uptake studies, 200 nM of labeled α S WT or α S-H50-HNE samples was incubated with cells (24 hours). To study the colocalization with lysosomes, the cells were treated with 75 nM LysoTracker Deep Red (Life Technologies, Carlsbad, CA) 1 hour before imaging.

Results and Discussion

HNE reaction with α S

HNE Modification of α S

A previous study showed that singly-modified HNE-modified α S can be produced depending on the concentration of HNE introduced to α S.²² To measure the appropriate level of HNE needed to maximize the yield of H50-HNE modified α S monomers, it was important to test various concentrations of HNE with α S WT. Thus, various molar ratios of α S: HNE were explored to find the appropriate amount of HNE needed for single Michael addition adducts ($\Delta+156$ m/z). **Figure 4** shows mass changes of α S corresponding to the various molar ratios of α S:HNE mixed at 37 °C overnight. When HNE was added to α S WT at a protein:HNE ratio of 1:2, only the α S WT mass (14460 m/z) was observed and the Michael addition adduct (14616 m/z) signal is hardly observed (**Figure 4A**). The Michael addition adduct signal gradually increased as more HNE was added, meaning that the Michael Addition adduct mass signal correlated with the amount of HNE introduced to α S for an overnight reaction (**Figure 4B-E**). As a result, 1:6 or 1:10 α S:HNE molar ratio showed high Michael addition adduct signal, making that molar ratio range desirable for an overnight reaction (**Figure 4C-D**). While **Figure 4E** does have a high single Michael addition adduct signal, it also had an additional unnecessary Michael addition adduct peak (14772 m/z), implying that HNE has reacted at multiple sites.

Separation of HNE-modified α -synuclein through HPLC

After establishing the appropriate amount of HNE needed for HNE-H50 modification, it was important to determine whether α S-H50-HNE monomers with a single Michael addition can be isolated and purified using HPLC. To purify the α S-H50-HNE monomers for biochemical studies, the HNE-reacted α S was injected into the Varian HPLC for separation. MALDI-MS shows HNE Michael addition adducts ($\Delta+156$) (**Figure 5A**). After injection into the Varian HPLC, distinct peaks of each modified α S could be separated, as two differentiated peaks are shown in the HPLC chromatogram (**Figure 5B**). The later peak (elution time=35 min) corresponds to the elution of α S-H50-HNE monomers (single Michael addition adduct) (**Figure 5B**). This meant that the fractions of only single-modified α S were able to be separated using HPLC. The MALDI-MS confirmed the identity and purity of α S-H50-HNE monomers (**Figure 5C**). Therefore, the isolation of α S-H50-HNE monomers supported the possibility of further investigating the site-specific effects of H50-HNE on α S biochemical properties.

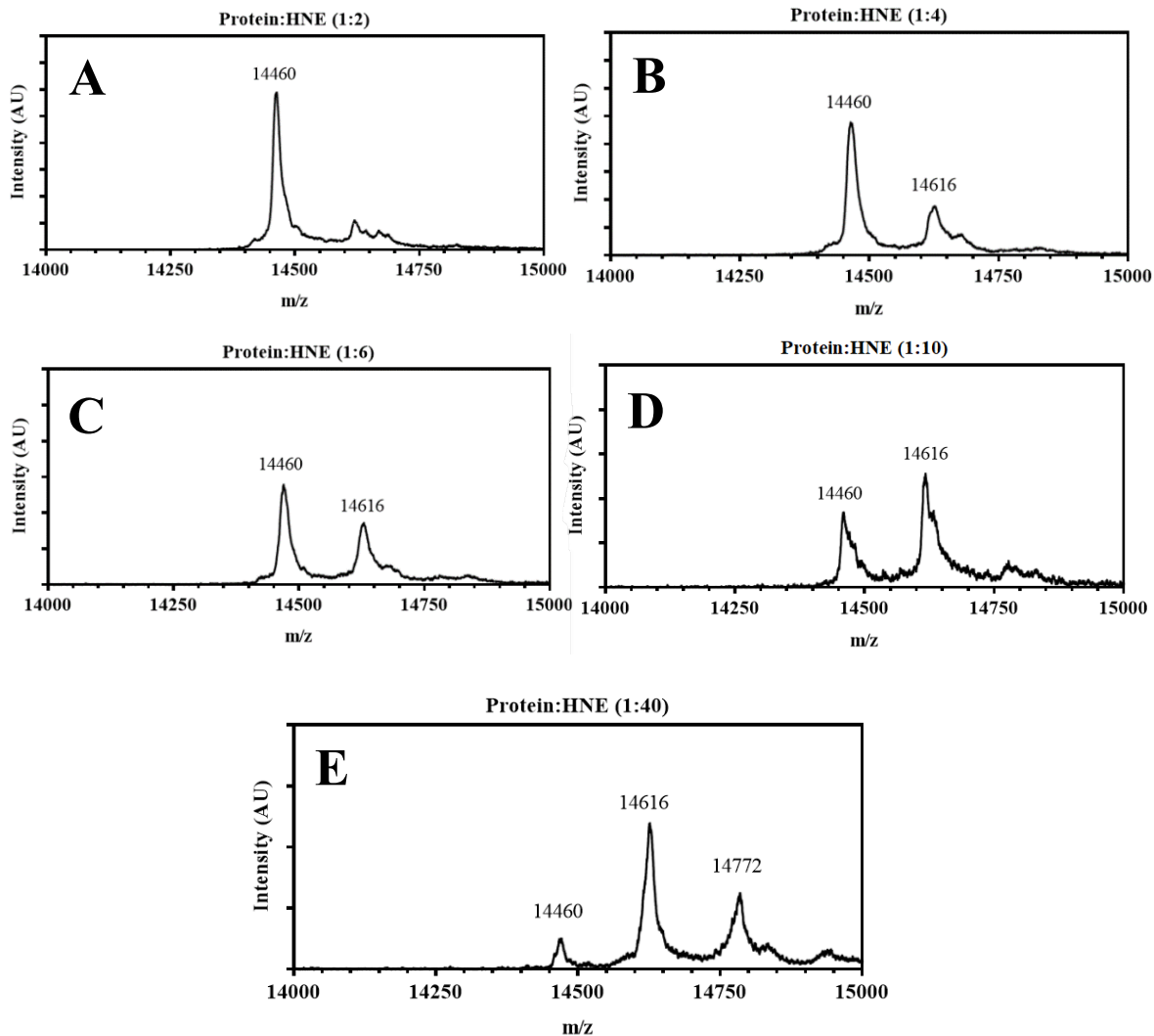


Figure 4. Different Concentrations of HNE reacted with α S at 37 °C overnight. MALDI-MS masses obtained for protein:aldehyde concentration ratios of (A) 1:2, (B) 1:4, (C) 1:6, (D) 1:10, and (E) 1:40.

Trypsin Digest of H50 modified α -synuclein

To verify the site-specific modification at H50, trypsin digest was performed on HNE-modified samples. It was expected that the single Michael addition on H50 for the 46-58 peptide would be observed on MALDI MS. However, MALDI MS showed four distinguishable peaks at 1433 m/z (46-58 peptide sequence with +138), 1451 m/z (46-58 peptide sequence with +156), 1662 m/z (46-60 peptide sequence with +138), and 1680 m/z (46-60 peptide sequence with +156) (**Figure 6A**), indicating the likelihood of a Schiff base reaction occurring on some of the peptides. Since α S-HNE-H50 showed only a Michael addition on a protein level, it is important to explore the possible reasoning

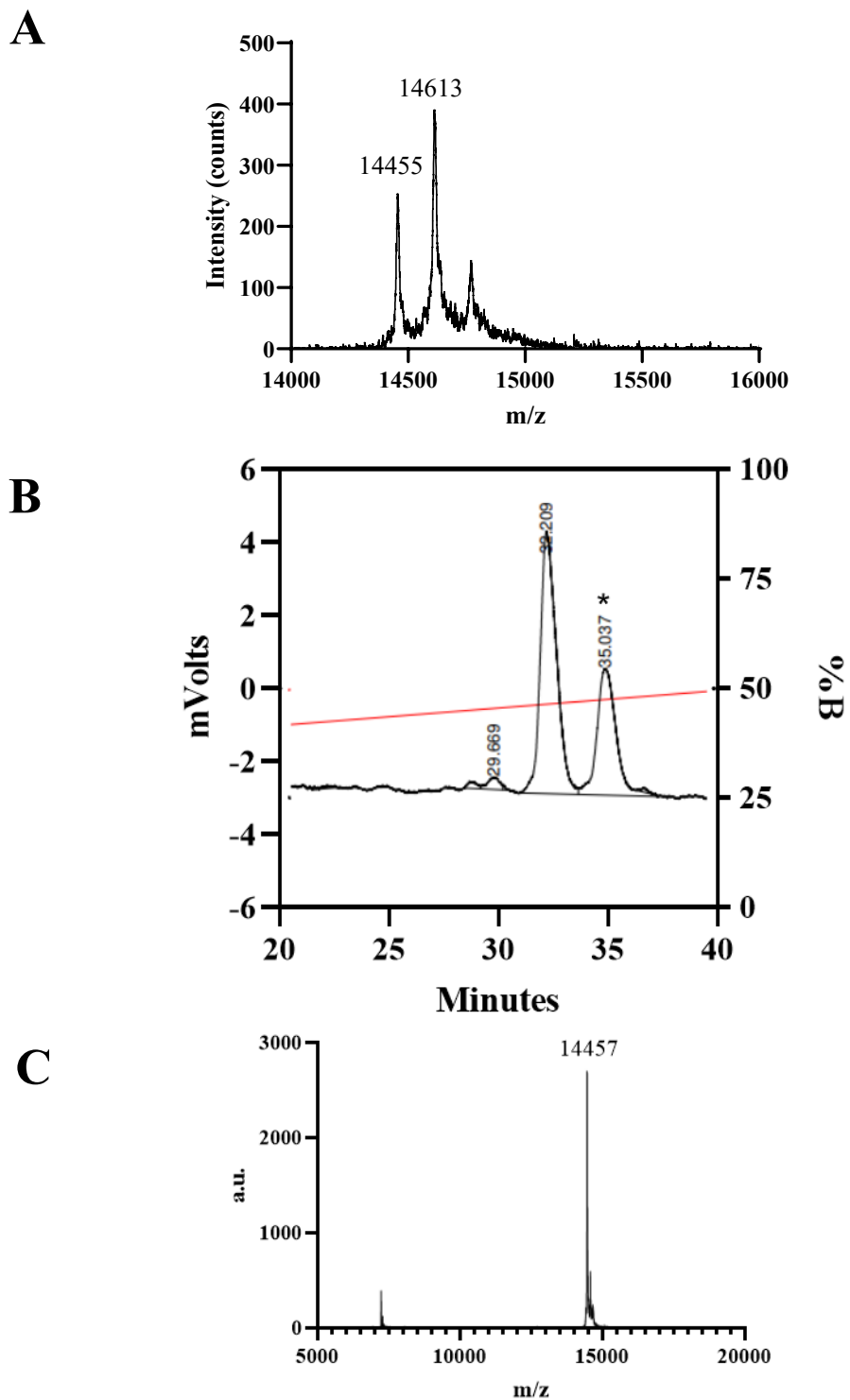


Figure 5. Separation of each HNE-modified α S. A) MALDI MS of HNE-modified α S is shown after overnight reaction. B) HPLC chromatogram of the HNE-modified α S at 215 nm (black) showing that separation of each HNE adduct is possible. C) MALDI-MS of the purified fractions of α S-H50-HNE monomers after HPLC.

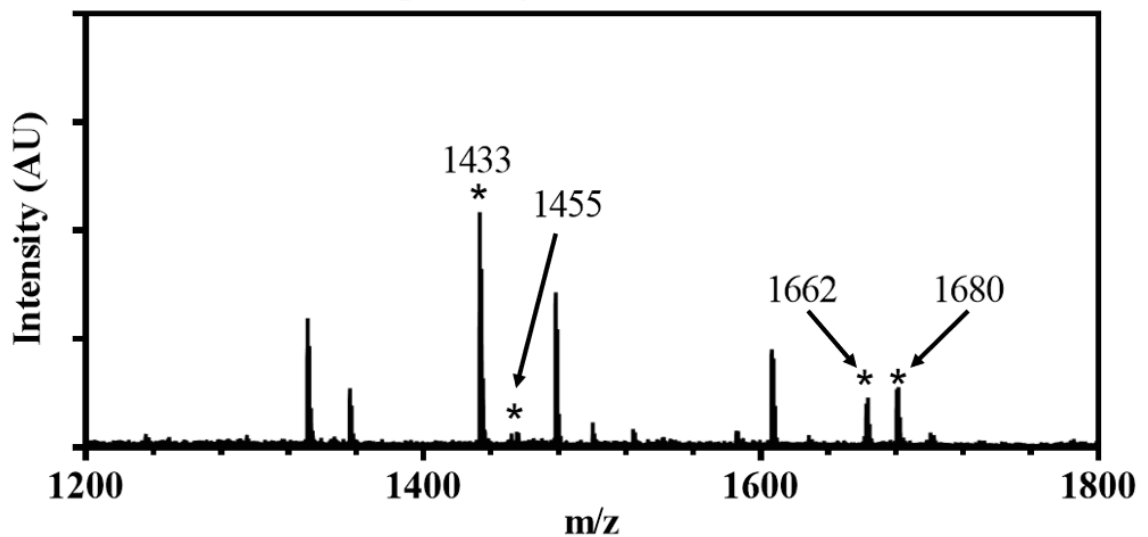
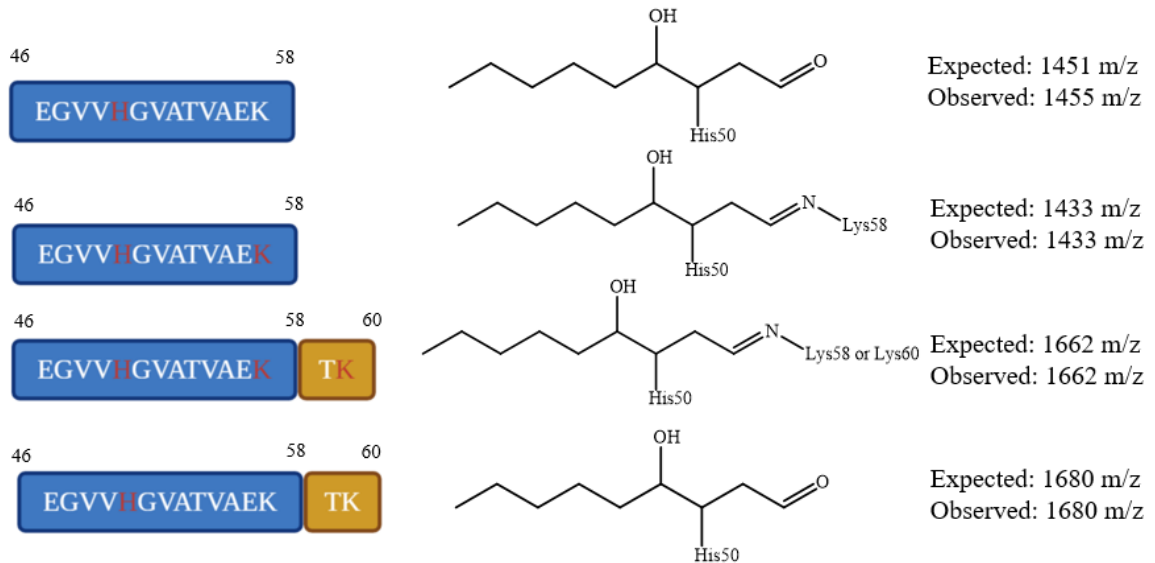
A**Trypsin Digest of α S-H50-HNE****B**

Figure 6. MALDI of Trypsin Digest peptides of H50-modified α S. A) The HNE-modified α S specifically at H50 underwent trypsin digest and yielded two important peaks. One peak is at 1433 m/z and the other is 106 m/z. These peaks showed a Schiff base modification (expected peptide+ Δ 138). B) The possible modification mechanism for the observed Schiff base mass change in part A. Red letters indicate the site of modification.

behind why some of the trypsin-digested peptides showed only Schiff base adducts. While the exact reason for this observed mass difference is not known, several studies have published results showing similar patterns. In one study, modification of Cytochrome C by HNE showed Michael addition ($\Delta+156$ m/z) on a protein level, but Schiff base reaction ($\Delta+138$ m/z) with trypsin-digested peptides of the same protein.³⁵ Similar results were observed in a study where they examined bovine serum albumin and lysozyme as models for HNE modifications.³⁶ Since the identified peptides include H50, it was unlikely that an retro-Michael addition has occurred. Rather, it is likely that both Michael addition and Schiff base reactions can occur simultaneously, where the Schiff base forms under trypsin digest conditions.

The mass peaks of 1433 m/z (46-58 peptide sequence with +138) and 1662 m/z (46-60 peptide sequence with +138) could correspond to Schiff base reaction of HNE with K58 or K60 and H50-HNE Michael addition (**Figure 6B**). The acidic conditions of trypsin digest could favor Schiff base formation and intramolecular trapping through the pre-existing H50-HNE bond would favor this cyclization. Trypsin digest for double HNE addition on α S was also explored, but it was unable to identify any other modifications. This may mean that the addition HNE reactions with the lysine residues may be random and do not have a preferential reactivity towards a specific lysine residue, leading to the difficulty of trying to identify the second HNE modification on α S. These data also support simultaneous Schiff base and Michael adduct formation, as Michael adduct dissociation and reformation of a separate Schiff base would be unlikely to occur only on the fragment with H50. Thus, the trypsin digest analysis largely confirms the first HNE modification site to be H50.

Characterization of α S Aggregation

Congo Red Aggregation Assay and α S incorporation assay

While HNE-modified α S is expected to form only oligomers based on studies by Xiang²⁸, it was uncertain whether α S-H50-HNE monomers would have the same aggregation patterns as a unpurified HNE-modified α S. If α S-H50-HNE monomers alone could inhibit fibril formation, this may signify that H50-HNE interaction alone plays an important role in aggregation and require the reexamination of how aldehydes affect the biophysical properties of α S.

To evaluate the effects of H50-HNE adduction on the aggregation of α S, Congo Red aggregation assays were performed. The identity and purity of the samples were confirmed using MALDI-MS (**Figure 7**). **Figure 7A** only showed the mass of α S WT (14457 m/z), and **Figure 7B** only showed the mass of α S-H50-HNE monomers (14613 m/z). Since the samples corresponded only to the expected masses, this eliminated any possibility that other impurities may affect aggregation.

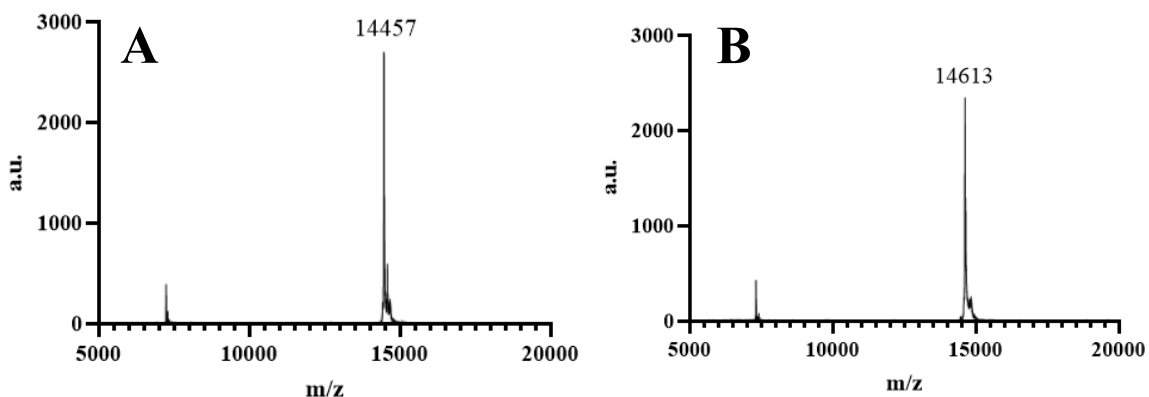


Figure 7. MALDI masses of α S samples before starting aggregation experiment. (A) α S WT. Expected mass of α S WT is 14460 m/z. (B) α S H₅₀-HNE. Expected mass of α S H₅₀-HNE is 14616 m/z.

The Congo Red aggregation assay was performed on two types of samples: α S WT (Control) and α S H₅₀-HNE (Experimental). Under aggregation conditions, Congo Red absorbance at 540 nm and 480 nm were measured at each timepoint to monitor the aggregation process. Since Congo Red is known to have high binding affinity towards amyloids, it can be expected that the absorbance signal will increase as aggregation occurs before reaching saturation. **Figure 8** shows the plot of Congo Red absorbance (540 nm/480 nm) at each timepoint (0, 4, 6, 8, 10, 12, 24, 28, 32, 36, 48, and 60 hours) for α S WT (Blue curve) and α S H₅₀-HNE (Red curve). The aggregation curve for α S WT was sigmoidal where the nucleation phase showed a rapid increase in Congo Red absorbance signal over time, and saturated around absorbance 1.2 at 12-16 hours, indicating that α S fibrils were fully formed around 12 hours (**Figure 8**). Meanwhile, the α S-H₅₀-HNE showed a flatter sigmoidal curve where nucleation phase had a much slower increase in Congo Red absorbance signal over time, and a much lower saturation point after 60 hours (**Figure 8**). In fact, the α S-H₅₀-HNE did not even reach absorbance 1.0, suggesting a possible alteration to the structural or aggregation properties of α S. The $T_{1/2}$ (half-life time) was 8.56 ± 0.24 hours for α S WT and 17.70 ± 1.29 hours for α S H₅₀-HNE, showing a significant difference in aggregation kinetics (**Figure 8**) After 60 hours, MALDI-MS revealed that α S-H₅₀-HNE samples had both α S WT and α S H₅₀-HNE adducts since both α S WT mass (14456 m/z) and α S-H₅₀-HNE mass (14613) was observed (**Figure 9**). This contrasts with the MALDI-MS before the experiments started where no α S WT peaks could be found in the α S H₅₀-HNE sample (**Figure 7**), indicating the possibility of a retro-Michael addition at H50 under aggregation conditions. This may indicate that there are some conditions where Michael addition adducts may be reversible.

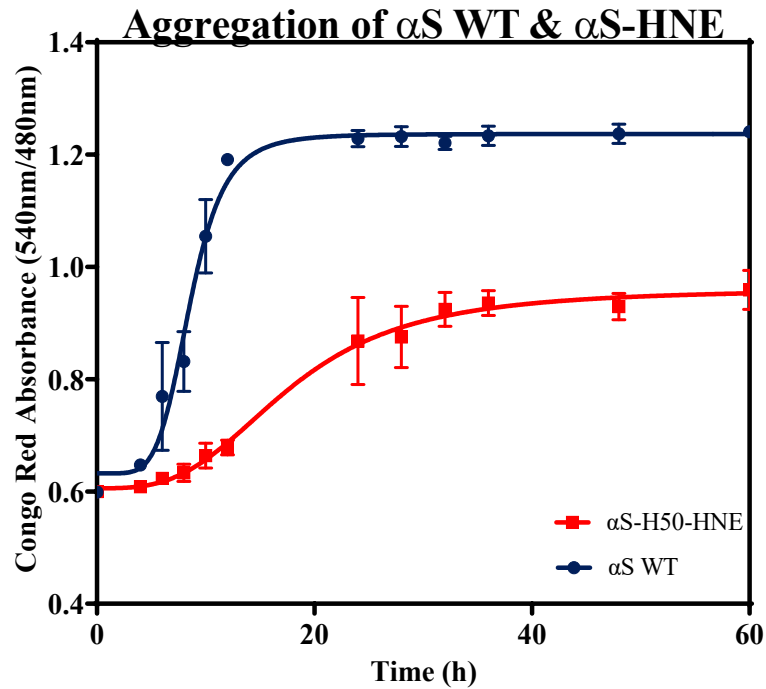


Figure 8. Congo Red Aggregation Assay for α S WT and α S-H50-HNE. Absorbances at 480 nm and 540 nm was measured at timepoints 0, 4, 6, 8, 10, 12, 24, 28, 32, 36, 48, and 60 hours. The $T_{1/2}$ is 8.56 ± 0.24 hours for α S WT and 17.70 ± 1.29 hours for α S H50-HNE. Red line indicates α S-H50-HNE aggregation and blue line indicates α S WT aggregation.

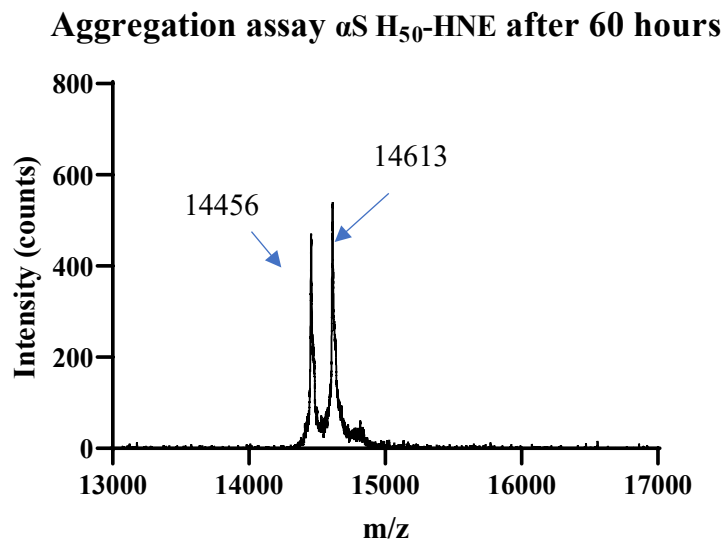


Figure 9. MALDI-MS showing the masses of the α S-H₅₀-HNE sample at 60-hour timepoint. Both α S WT (14456 m/z) and α S-H₅₀-HNE (14613 m/z) masses are observed.

α S incorporation assay

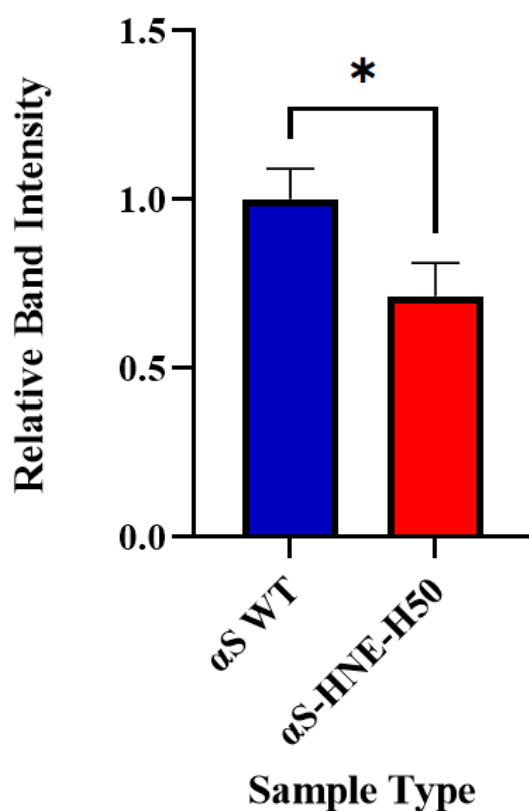


Figure 10. Quantification of α S incorporated in fibrils and aggregates with SDS-PAGE. The relative band intensity of α S samples were measured and compared between α S WT and α S-HNE modified samples (* p <0.05).

To quantify the amount of α S incorporated in the fibrils or aggregates, the aggregated α S were isolated, solubilized, and run on an SDS-PAGE gel. The band intensities were analyzed to quantify the relative amounts of α S incorporated in aggregated samples. **Figure 10** shows the relative band intensity of α S WT and α S-H50-HNE, meaning the relative amount of α S incorporated in the aggregates can be compared for each sample. When the band intensities were quantified, there was a significant difference (* p <0.05) between the amount of α S incorporated in α S WT aggregates and the amount of α S incorporated in α S-H50-HNE aggregates, as α S-H50-HNE showed a much lower α S relative band intensity than that of α S WT (**Figure 10**).

Cryo-EM studies have shown that H50 and E57 form a salt bridge, which is at the core of α S fibril formation.⁸ Mutational studies have also shown that HNE-mediated toxicity disappears after mutating H50.^{22, 29} It was predicted that HNE could interfere with this interaction and change how fibrils are formed. The aggregation assay and α S incorporation assay data in this report show that HNE modification at H50 clearly impeded its ability to form fibrils. This may mean that HNE prevented the formation of a salt bridge between H50 and E57 required to make efficient fibrils. Moreover, this might

suggest that a single modification at H50 is enough to completely change its aggregation properties and structure-based biotoxicity, contradicting the original beliefs about how oligomerization is necessary for fibril prevention and toxicity. Therefore, it was necessary to explore the amount of α S incorporation and the cluster size of aggregated samples.

Dynamic light scattering (DLS) analysis of α s aggregated samples

The samples that were under aggregation conditions for 60 hours were analyzed on DLS for size analysis. Since DLS can determine the size of a sample particle, the rationale was that DLS will be able to determine how the size of the aggregates are affected by HNE. It is expected that α S WT particles have a larger average size since Congo Red assay and α S incorporation experiments have showed faster aggregation kinetics and higher α S content for α S WT fibril samples. **Figure 11A** shows the size distribution of α S WT fibrils (3 measurements named α S WT 1, 2, and 3), which all had a size around 1000 d.nm (diameter nm). **Figure 11B** represent the size distribution of α S-H50-HNE aggregated (3 measurements named α S-H50-HNE 1, 2, and 3), which all had a size slightly below 1000 d.nm (diameter nm). **Figure 11C** shows both **Figure 11A** and **Figure 11B** for better comparison, which indicated that the size of the α S-H50-HNE aggregates were slightly smaller than the size of the α S fibrils. The comparison of the samples clearly shows this small difference in size since α S-H50-HNE peaks are slightly shifted to the left side of the α S WT fibrils (**Figure 11C**). This observation led to two possible implications: 1) HNE-H50 interaction may lead to smaller α S aggregates and 2) these aggregates are not likely α S oligomers, which are favorably stabilized in excess HNE.²² It is uncertain whether these smaller aggregates represent fibril intermediates from HNE-dissociated α S, but it is obvious that alteration of H50 can dictate the structural and interactive dynamics of α S. It may be interesting to characterize the conformational structure of the aggregates with transmission electron microscopy or cryo-EM since the DLS can only confirm the overall bulk of the aggregates.

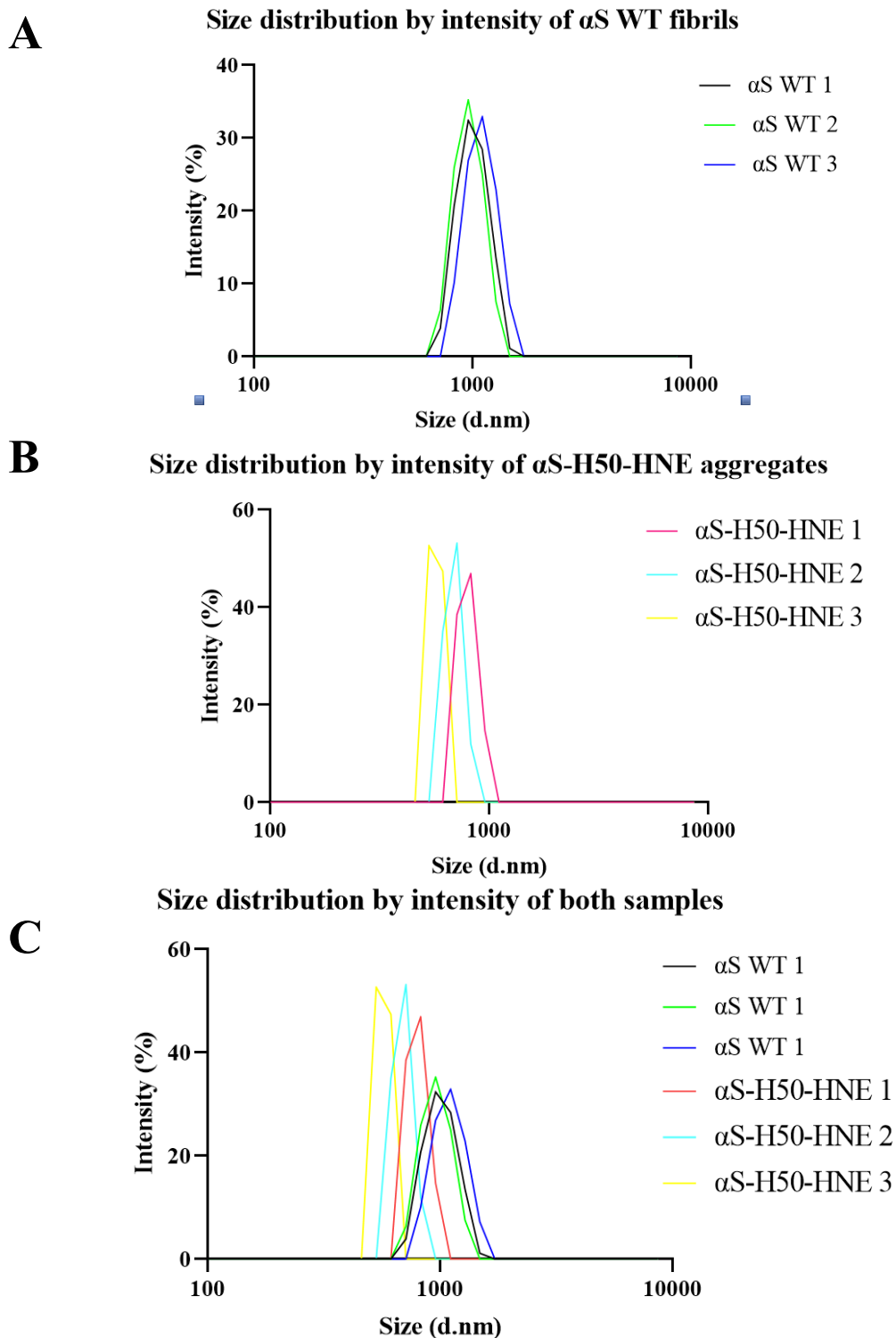


Figure 11. DLS of α S WT fibrils and α S HNE-modified aggregates. The size distribution by intensity represents the (A) three sample measurements of α S WT and (B) three sample measurements of α S-H50-HNE after aggregation. (C) The size distribution of both samples integrated on same plot are shown for comparison.

Measurement of α S lipid binding

Expression and Purification of α -synuclein PpY114

The Petersson lab had previously engineered a way to site-specifically incorporate PpY on α S using unnatural amino acid mutagenesis.^{31, 32, 37} This method was preferred over cysteine labeling since cysteine can interact with HNE and disrupt the desired HNE modification on H50. In this case, propargyl tyrosine (PpY) with a reactive handle for alkyne was incorporated into α S so that it can function as a reactive handle for alkyne-azide click chemistry. Position 114 was selected for PpY incorporation because it was located in a region not involved in lipid binding or aggregation.³⁸ The incorporation of PpY at position 114 was accomplished via amber codon suppression. α S-PpY114 was expressed using a α S construct fused with a C-terminal intein tag. The intein tag was later cleaved with BME and the α S PpY114 was later purified with the FPLC. The purified α S PpY114 was confirmed using MALDI-MS (**Figure 12**).

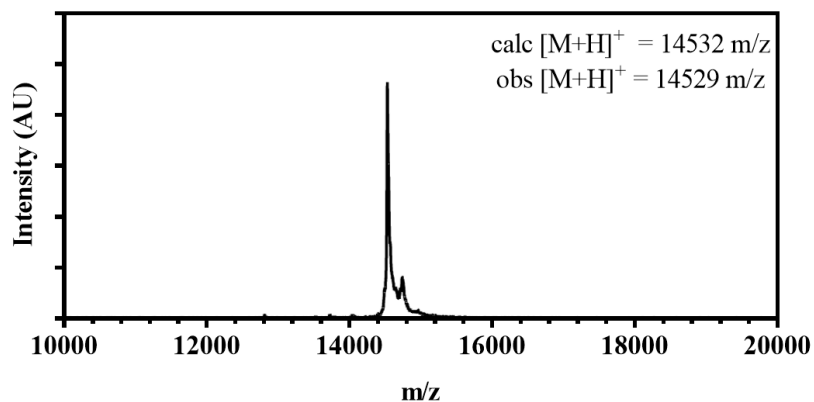


Figure 12. Purification of α S PpY114. The observed mass (14528 m/z) corresponded to the expected mass (14532 m/z) of α S PpY114.

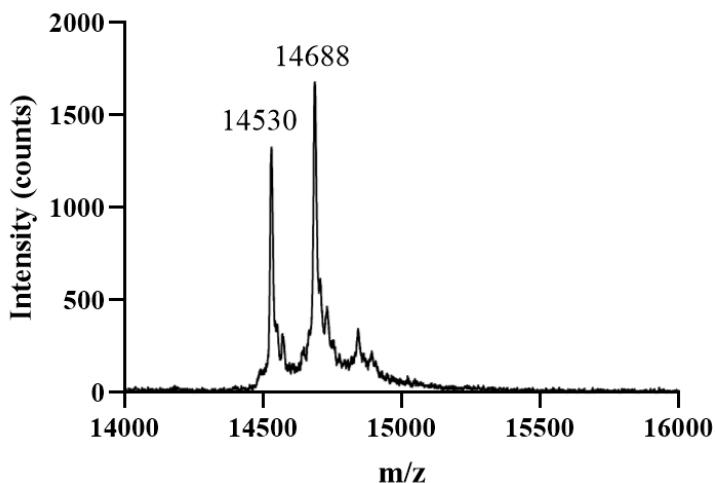


Figure 13. HNE-modification to α S PpY114. The highlighted peak mass (14686 m/z) matches the expected mass for HNE-modified mass (14688 m/z).

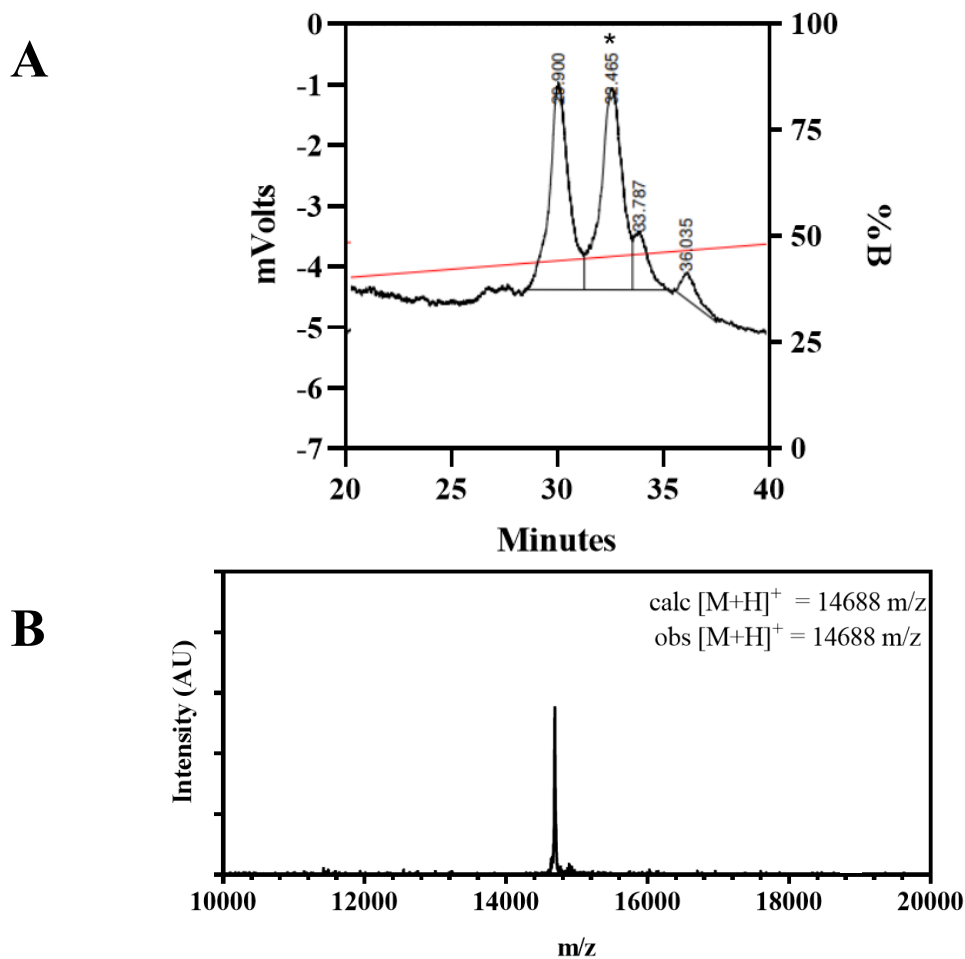


Figure 14. HPLC Purification of H50 HNE-modified α S PpY114. (A) HPLC chromatogram of the HNE-reacted α S PpY114 for which MALDI-MS is shown. (B) The purified samples of HNE reacted with H50 α S were confirmed with MALDI-MS. The observed masses (14688 m/z) matched the expected mass of HNE-modified α S.

HNE modification of α S PpY114

Using the same method to react HNE with α S WT, α S PpY114 was also reacted with HNE. After purifying α S PpY114 on the FPLC, the samples were reacted with HNE overnight to yield a single Michael addition adduct at H50, which the mass (14686 m/z) was confirmed on the MALDI-MS (**Figure 13**). To purify only α S with a single HNE modification at H50, the reacted sample was injected onto Varian HPLC. **Figure 14A** shows the HPLC chromatogram at 215 nm where the HNE-modified α S PpY114 was eluted at the later peak (elution time=32 min). Afterwards, the purity of HNE-modified α S PpY114 was confirmed with MALDI-MS since the 14688 mass was observed (**Figure 14B**). Therefore, the results showed that it was possible to isolate HNE-modified α S with PpY incorporated at position 114.

Labeling of HNE-modified α -synuclein with Atto488

Following the reaction of HNE and α S-PpY114, the click chemistry labeling of PpY114 alkyne with Atto488-azide was achieved in the presence of a copper catalyst.⁶ This mixture was injected onto the HPLC for purification. To confirm that α S-PpY114 was labeled correctly with Atto488-azide, the reaction product mass (15486 m/z) was analyzed through MALDI-MS and matched the expected mass (15478 m/z) (**Figure 15**). This demonstrated that it was possible to label HNE-modified α S without having the HNE interfere in the process, meaning the labeled protein can be used as a probe to monitor vesicle binding and uptake in cell studies.

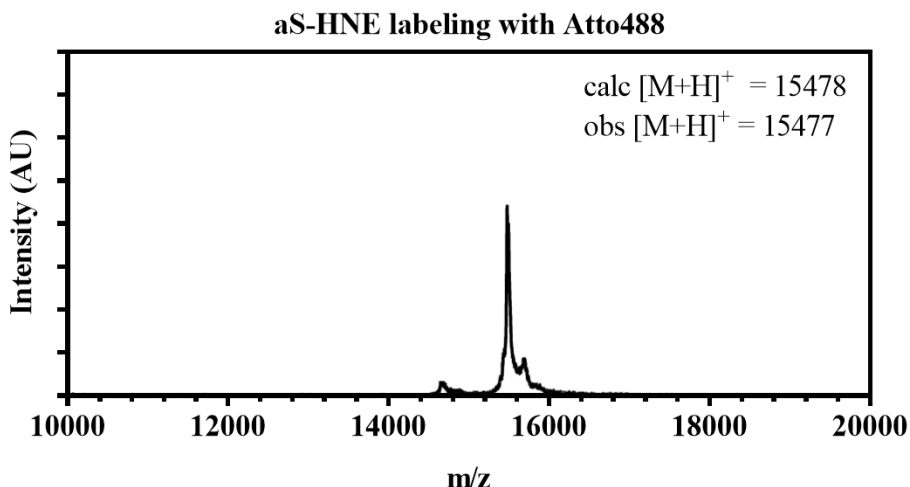


Figure 15. MALDI-MS data of HNE-modified α S PpY114 labeled with Atto488-azide after HPLC purification. The observed mass (15477 m/z) matches the expected mass (15478 m/z).

The effects of HNE-modified α S on lipid vesicle binding

Using the samples labeled with Atto488, the vesicle binding affinity of α S-HNE was explored with FCS. At a constant α S concentration, the FCS data were collected with increasing lipid concentrations. The autocorrelation curves were fit to **Equation 2** to calculate the amount of lipid bound and free α S. Thus, **Figure 16** presents the fraction of bound α S plotted as a function of increasing lipid concentration, which allows direct comparison of lipid binding affinity. α S WT (black) and HNE-modified α S (green) samples were incubated with POPS/POPC (50:50) lipid vesicles, and the amount of α S bound to lipid vesicle was measured at each lipid concentration. For higher binding affinity, it is expected that the fraction of α S bound to lipids will reach 1.0 at lower lipid concentrations. **Figure 16** shows that α S-H50-HNE had a stronger binding affinity towards lipids than that of α S WT, since the α S-H50-HNE reached 1.0 at a lower vesicle concentration (**Figure 16**). By applying **Equation 3** to calculate the binding affinity ($K_{d, app}$), the results showed that the calculated binding affinity ($K_{d, app}$) was $10.7 \pm 1.4 \mu\text{M}$ for

α S WT and $5.7 \pm 0.9 \mu\text{M}$ for α S-H50-HNE, meaning α S-H50-HNE leads to a two-fold increase in vesicle binding.

It is unlikely that this result is solely due to a positional or conformational effect, since H50Q mutation did not significantly affect the conformational structure or lipid binding affinity of α S.³⁹ This may mean that the chemical properties of the modification might dictate its increased binding affinity towards lipid vesicles. Although there is no data on how α S-H50-HNE affects lipid vesicle binding, several studies have implicated several possibilities. One possibility is that HNE may directly interact with phospholipids and may undergo a Michael Addition/Schiff Base reaction.⁴⁰ Since HNE is highly reactive, it is unsurprising to expect such reactions to happen with phospholipid. However, further studies need to establish the stability and reversibility of such reactions in various conditions before this conclusion can be made.

Another possibility may be related to the amphipathic nature of α S. It is generally known that the long amphipathic α -helical structure is crucial for membrane bounding. A study from Braun found that the seven imperfect 11-mer repeats play an important role in the amphipathic nature of α S and truncation of this region led to a 15% decrease in lipid binding affinity.⁴¹ Additionally, molecular dynamics simulations showed that HNE may be stably bound in the carbonyl region of the POPC bilayer.⁴² The aldehyde and hydroxyl group were found to reside towards the carbonyl groups of POPC lipid molecules, while the aliphatic tail of HNE was located along with other aliphatic tails from POPC. In other words, the amphiphilic character of HNE may enhance its stabilization in the lipid bilayer by both hydrophobic interactions between HNE hydrocarbon chain and aliphatic tails of lipids and polar interactions between the polar groups of HNE and the headgroups of lipids. Therefore, the implication is that H50-HNE modification enhances the amphipathic nature of α S and may induce the α -helical characteristics of α S, leading to a stronger binding affinity towards phospholipid membranes. A similar study done with acetylated α S confirmed the increased lipid binding where a longer α -helical structure can lead to a better binding affinity.⁴³ Consequentially, this may explain why HNE modification promote higher binding affinity towards lipid vesicles.

Regardless, both possibilities might implicate that HNE-modified α S can contribute to the permeabilization of lipid and cell membranes. It has been shown that HNE-induced α S oligomers can permeabilize DOPG vesicles.⁴⁴ Despite its reactivity towards lipid vesicles, HNE is expected to have little to no effect on the properties of lipid bilayers, such as membrane thickness and area per lipid under physiological conditions.⁴² Also, based on the raw diffusion time signal of α S-H50-HNE monomers, there were no indication of a vesicle structure disruption. However, this may change when larger HNE bioparticles bind with lipid bilayers, potentially causing permeabilization observed with HNE-modified α S oligomers. Therefore, it might be possible that the amphiphilic nature of HNE may play a role in its α S-mediated toxicity.

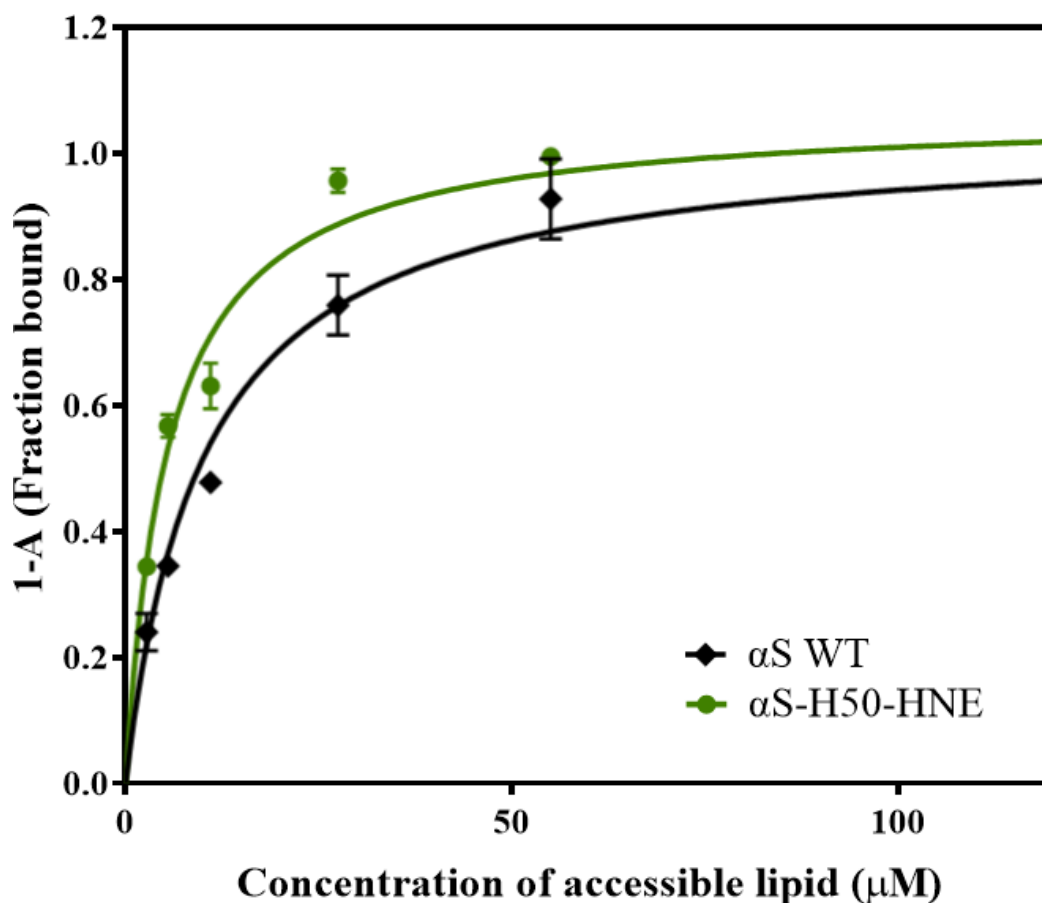


Figure 16. The binding affinity of α S WT and α S-H50-HNE samples on lipid vesicles. POPS/POPC (50:50) were mixed with both samples. The binding affinity ($K_{d, app}$) of α S WT was $10.7 \pm 1.4 \mu\text{M}$ and $5.7 \pm 0.9 \mu\text{M}$. The green line indicates α S-H50-HNE samples and black line indicates α S WT samples.

Cell uptake and internalization studies

The effects of HNE-modified α S on SH-SY5Y cells

To learn if HNE-modified α S monomers can affect cell uptake, the labeled α S-H50-HNE monomers were introduced to SH-SY5Y cells. Although the exact role of HNE-modified α S in cell uptake and internalization is not fully established, some studies have suggested that HNE-induced α S oligomers might increase cell uptake and cell-to-cell transfer, indicating a possibility that the reactive ability of HNE might help permeabilize cell membranes and bilayers for better uptake.^{45, 46} This raises an important question whether HNE modification can increase cell uptake or cell-to-cell transmission. Also, it was predicted that α S-H50-HNE monomers will internalize within the endosomal/lysosomal system since past studies have shown HNE-modified and other PTM-modified α S can localize in those regions.⁴⁶ This may mean that the HNE-modified α S may be involved in the lysosomal system or pathway. In **Figure 17**, the images show SH-SY5Y cells that have been exposed to fluorescently labeled α S WT or α S-H50-HNE samples. Since both α S WT and α S-H50-HNE were labeled with Atto488, those components are observed in

Conclusion

In conclusion, this report studied the site-specific HNE modification of α S H50 and its effect on the biophysical properties of α S. The α S monomers with the site-specific interaction of H50 and HNE were successfully isolated using HPLC. This isolation allowed for further experiments that explored the specific effects of the H50-HNE interaction on aggregation, lipid binding, and cell uptake. Congo Red assay, α S incorporation assay, and DLS experiments showed a significant decrease in aggregation kinetics and aggregate sizes when H50 was modified with HNE. This may indicate that the single HNE modification on H50 can change the aggregation patterns or size of α S aggregates, although its structural relevance to α S pathology is yet to be established. Structural characterization techniques such as Cryo-EM or TEM might shed more light on how the site-specific modification changes the aggregation process. Also, it was observed that the H50-HNE Michael addition can undergo dissociation in aggregation conditions, proving the reversibility of this specific reaction. Lipid binding experiments showed a two-fold increase in lipid binding affinity for α S-H50-HNE samples ($5.7 \pm 0.9 \mu\text{M}$) compared to the lipid binding affinity of α S WT ($10.7 \pm 1.4 \mu\text{M}$). This increase in lipid membranes might propose an important role in α S function, possibly influencing neurotransmission release and synaptic function in dopaminergic synapses. Preliminary cell studies showed that both α S WT and α S-H50-HNE monomers resulted in very little uptake. However, when uptake was observed, both α S WT and α S-H50-HNE monomers internalized in the lysosomal region, implicating its potential participation in the lysosomal/endosomal pathway. However, further experiments are needed to assess the accuracy of these cell study results. Together, the report showed that the H50-HNE interaction alone can significantly change the biophysical properties of α S, highlighting the potential role it may have in α S function or pathology.

References

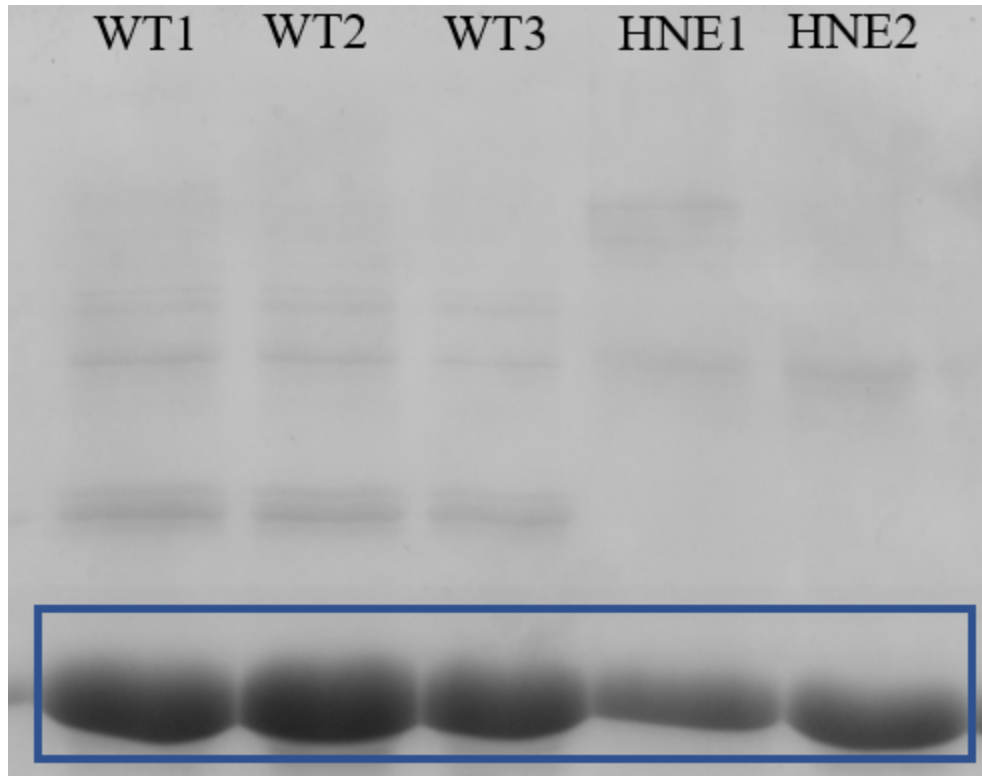
1. Spillantini, M. G.; Schmidt, M. L.; Lee, V. M. Y.; Trojanowski, J. Q.; Jakes, R.; Goedert, M., alpha-synuclein in Lewy bodies. *Nature* **1997**, *388* (6645), 839-840.
2. Spillantini, M. G.; Crowther, R. A.; Jakes, R.; Hasegawa, M.; Goedert, M., alpha-synuclein in filamentous inclusions of Lewy bodies from Parkinson's disease and dementia with Lewy bodies. *P Natl Acad Sci USA* **1998**, *95* (11), 6469-6473.
3. Giasson, B. I.; Murray, I. V.; Trojanowski, J. Q.; Lee, V. M., A hydrophobic stretch of 12 amino acid residues in the middle of alpha-synuclein is essential for filament assembly. *J Biol Chem* **2001**, *276* (4), 2380-6.
4. Uversky, V. N.; Eliezer, D., Biophysics of Parkinson's disease: structure and aggregation of alpha-synuclein. *Curr Protein Pept Sci* **2009**, *10* (5), 483-99.
5. Nemani, V. M.; Lu, W.; Berge, V.; Nakamura, K.; Onoa, B.; Lee, M. K.; Chaudhry, F. A.; Nicoll, R. A.; Edwards, R. H., Increased expression of alpha-synuclein reduces neurotransmitter release by inhibiting synaptic vesicle reclustering after endocytosis. *Neuron* **2010**, *65* (1), 66-79.
6. Perez, R. G.; Waymire, J. C.; Lin, E.; Liu, J. J.; Guo, F.; Zigmond, M. J., A role for alpha-synuclein in the regulation of dopamine biosynthesis. *J Neurosci* **2002**, *22* (8), 3090-9.
7. Al-Wandi, A.; Ninkina, N.; Millership, S.; Williamson, S. J.; Jones, P. A.; Buchman, V. L., Absence of alpha-synuclein affects dopamine metabolism and synaptic markers in the striatum of aging mice. *Neurobiol Aging* **2010**, *31* (5), 796-804.
8. Cooper, A. A.; Gitler, A. D.; Cashikar, A.; Haynes, C. M.; Hill, K. J.; Bhullar, B.; Liu, K.; Xu, K.; Strathearn, K. E.; Liu, F.; Cao, S.; Caldwell, K. A.; Caldwell, G. A.; Marsischky, G.; Kolodner, R. D.; Labeaer, J.; Rochet, J. C.; Bonini, N. M.; Lindquist, S., Alpha-synuclein blocks ER-Golgi traffic and Rab1 rescues neuron loss in Parkinson's models. *Science* **2006**, *313* (5785), 324-8.
9. Sun, J.; Wang, L.; Bao, H.; Premi, S.; Das, U.; Chapman, E. R.; Roy, S., Functional cooperation of alpha-synuclein and VAMP2 in synaptic vesicle recycling. *Proc Natl Acad Sci U S A* **2019**, *116* (23), 11113-11115.
10. Scott, D.; Roy, S., alpha-Synuclein inhibits intersynaptic vesicle mobility and maintains recycling-pool homeostasis. *J Neurosci* **2012**, *32* (30), 10129-35.
11. Chandra, S.; Gallardo, G.; Fernandez-Chacon, R.; Schluter, O. M.; Sudhof, T. C., Alpha-synuclein cooperates with CSPalpha in preventing neurodegeneration. *Cell* **2005**, *123* (3), 383-96.
12. Schaser, A. J.; Osterberg, V. R.; Dent, S. E.; Stackhouse, T. L.; Wakeham, C. M.; Boutros, S. W.; Weston, L. J.; Owen, N.; Weissman, T. A.; Luna, E.; Raber, J.; Luk, K. C.; McCullough, A. K.; Woltjer, R. L.; Unni, V. K., Alpha-synuclein is a DNA binding protein that modulates DNA repair with implications for Lewy body disorders. *Sci Rep* **2019**, *9* (1), 10919.
13. Zhu, M.; Qin, Z. J.; Hu, D.; Munishkina, L. A.; Fink, A. L., Alpha-synuclein can function as an antioxidant preventing oxidation of unsaturated lipid in vesicles. *Biochemistry* **2006**, *45* (26), 8135-42.
14. Barbour, R.; Kling, K.; Anderson, J. P.; Banducci, K.; Cole, T.; Diep, L.; Fox, M.; Goldstein, J. M.; Soriano, F.; Seubert, P.; Chilcote, T. J., Red blood cells are the major source of alpha-synuclein in blood. *Neurodegener Dis* **2008**, *5* (2), 55-9.
15. Halliday, G. M., Re-evaluating the glio-centric view of multiple system atrophy by highlighting the neuronal involvement. *Brain* **2015**, *138* (Pt 8), 2116-9.
16. Zhang, J.; Li, X.; Li, J. D., The Roles of Post-translational Modifications on alpha-Synuclein in the Pathogenesis of Parkinson's Diseases. *Front Neurosci* **2019**, *13*, 381.
17. Anderson, J. P.; Walker, D. E.; Goldstein, J. M.; de Laat, R.; Banducci, K.; Caccavello, R. J.; Barbour, R.; Huang, J.; Kling, K.; Lee, M.; Diep, L.; Keim, P. S.; Shen, X.;

- Chataway, T.; Schlossmacher, M. G.; Seubert, P.; Schenk, D.; Sinha, S.; Gai, W. P.; Chilcote, T. J., Phosphorylation of Ser-129 is the dominant pathological modification of alpha-synuclein in familial and sporadic Lewy body disease. *J Biol Chem* **2006**, *281* (40), 29739-52.
18. Fujiwara, H.; Hasegawa, M.; Dohmae, N.; Kawashima, A.; Masliah, E.; Goldberg, M. S.; Shen, J.; Takio, K.; Iwatsubo, T., alpha-Synuclein is phosphorylated in synucleinopathy lesions. *Nat Cell Biol* **2002**, *4* (2), 160-4.
19. Hasegawa, M.; Fujiwara, H.; Nonaka, T.; Wakabayashi, K.; Takahashi, H.; Lee, V. M.; Trojanowski, J. Q.; Mann, D.; Iwatsubo, T., Phosphorylated alpha-synuclein is ubiquitinated in alpha-synucleinopathy lesions. *J Biol Chem* **2002**, *277* (50), 49071-6.
20. Csala, M.; Kardon, T.; Legeza, B.; Lizak, B.; Mandl, J.; Margittai, E.; Puskas, F.; Szaraz, P.; Szelenyi, P.; Banhegyi, G., On the role of 4-hydroxynonenal in health and disease. *Biochim Biophys Acta* **2015**, *1852* (5), 826-38.
21. Guillen, M. D.; Cabo, N.; Ibargoitia, M. L.; Ruiz, A., Study of both sunflower oil and its headspace throughout the oxidation process. Occurrence in the headspace of toxic oxygenated aldehydes. *J Agric Food Chem* **2005**, *53* (4), 1093-101.
22. Qin, Z.; Hu, D.; Han, S.; Reaney, S. H.; Di Monte, D. A.; Fink, A. L., Effect of 4-hydroxy-2-nonenal modification on alpha-synuclein aggregation. *J Biol Chem* **2007**, *282* (8), 5862-70.
23. Butterfield, D. A.; Bader Lange, M. L.; Sultana, R., Involvements of the lipid peroxidation product, HNE, in the pathogenesis and progression of Alzheimer's disease. *Biochim Biophys Acta* **2010**, *1801* (8), 924-9.
24. Mark, R. J.; Pang, Z.; Geddes, J. W.; Uchida, K.; Mattson, M. P., Amyloid beta-peptide impairs glucose transport in hippocampal and cortical neurons: involvement of membrane lipid peroxidation. *J Neurosci* **1997**, *17* (3), 1046-54.
25. Keller, J. N.; Pang, Z.; Geddes, J. W.; Begley, J. G.; Germeyer, A.; Waeg, G.; Mattson, M. P., Impairment of glucose and glutamate transport and induction of mitochondrial oxidative stress and dysfunction in synaptosomes by amyloid beta-peptide: role of the lipid peroxidation product 4-hydroxynonenal. *J Neurochem* **1997**, *69* (1), 273-84.
26. Castellani, R. J.; Perry, G.; Siedlak, S. L.; Nunomura, A.; Shimohama, S.; Zhang, J.; Montine, T.; Sayre, L. M.; Smith, M. A., Hydroxynonenal adducts indicate a role for lipid peroxidation in neocortical and brainstem Lewy bodies in humans. *Neurosci Lett* **2002**, *319* (1), 25-8.
27. Yoritaka, A.; Hattori, N.; Uchida, K.; Tanaka, M.; Stadtman, E. R.; Mizuno, Y., Immunohistochemical detection of 4-hydroxynonenal protein adducts in Parkinson disease. *Proc Natl Acad Sci U S A* **1996**, *93* (7), 2696-701.
28. Xiang, W.; Menges, S.; Schlachetzki, J. C.; Meixner, H.; Hoffmann, A. C.; Schlotzer-Schrehardt, U.; Becker, C. M.; Winkler, J.; Klucken, J., Posttranslational modification and mutation of histidine 50 trigger alpha synuclein aggregation and toxicity. *Mol Neurodegener* **2015**, *10*, 8.
29. Guerrero-Ferreira, R.; Taylor, N. M.; Mona, D.; Ringler, P.; Lauer, M. E.; Riek, R.; Britschgi, M.; Stahlberg, H., Cryo-EM structure of alpha-synuclein fibrils. *Elife* **2018**, *7*.
30. Boyer, D. R.; Li, B.; Sun, C.; Fan, W.; Sawaya, M. R.; Jiang, L.; Eisenberg, D. S., Structures of fibrils formed by alpha-synuclein hereditary disease mutant H50Q reveal new polymorphs. *Nat Struct Mol Biol* **2019**, *26* (11), 1044-1052.
31. Batjargal, S.; Walters, C. R.; Petersson, E. J., Inteins as traceless purification tags for unnatural amino acid proteins. *J Am Chem Soc* **2015**, *137* (5), 1734-7.
32. Haney, C. M.; Wissner, R. F.; Warner, J. B.; Wang, Y. J.; Ferrie, J. J.; D, J. C.; Karpowicz, R. J.; Lee, V. M.; Petersson, E. J., Comparison of strategies for non-perturbing labeling of alpha-synuclein to study amyloidogenesis. *Org Biomol Chem* **2016**, *14* (5), 1584-92.

33. Rhoades, E.; Ramlall, T. F.; Webb, W. W.; Eliezer, D., Quantification of alpha-synuclein binding to lipid vesicles using fluorescence correlation spectroscopy. *Biophys J* **2006**, *90* (12), 4692-700.
34. Daniels, M. J.; Nourse, J. B., Jr.; Kim, H.; Sainati, V.; Schiavina, M.; Murrall, M. G.; Pan, B.; Ferrie, J. J.; Haney, C. M.; Moons, R.; Gould, N. S.; Natalello, A.; Grandori, R.; Sobott, F.; Petersson, E. J.; Rhoades, E.; Pierattelli, R.; Felli, I.; Uversky, V. N.; Caldwell, K. A.; Caldwell, G. A.; Krol, E. S.; Ischiropoulos, H., Cyclized NDGA modifies dynamic alpha-synuclein monomers preventing aggregation and toxicity. *Sci Rep* **2019**, *9* (1), 2937.
35. Isom, A. L.; Barnes, S.; Wilson, L.; Kirk, M.; Coward, L.; Darley-Usmar, V., Modification of Cytochrome c by 4-hydroxy-2-nonenal: evidence for histidine, lysine, and arginine-aldehyde adducts. *J Am Soc Mass Spectrom* **2004**, *15* (8), 1136-47.
36. Aslebagh, R.; Pfeffer, B. A.; Fliesler, S. J.; Darie, C. C., Mass spectrometry-based proteomics of oxidative stress: Identification of 4-hydroxy-2-nonenal (HNE) adducts of amino acids using lysozyme and bovine serum albumin as model proteins. *Electrophoresis* **2016**, *37* (20), 2615-2623.
37. Haney, C. M.; Petersson, E. J., Fluorescence spectroscopy reveals N-terminal order in fibrillar forms of alpha-synuclein. *Chem Commun (Camb)* **2018**, *54* (7), 833-836.
38. Bussell, R., Jr.; Eliezer, D., A structural and functional role for 11-mer repeats in alpha-synuclein and other exchangeable lipid binding proteins. *J Mol Biol* **2003**, *329* (4), 763-78.
39. Khalaf, O.; Fauvet, B.; Oueslati, A.; Dikiy, I.; Mahul-Mellier, A. L.; Ruggeri, F. S.; Mbefo, M. K.; Vercruysse, F.; Dietler, G.; Lee, S. J.; Eliezer, D.; Lashuel, H. A., The H50Q mutation enhances alpha-synuclein aggregation, secretion, and toxicity. *J Biol Chem* **2014**, *289* (32), 21856-76.
40. Jovanovic, O.; Skulj, S.; Pohl, E. E.; Vazdar, M., Covalent modification of phosphatidylethanolamine by 4-hydroxy-2-nonenal increases sodium permeability across phospholipid bilayer membranes. *Free Radic Biol Med* **2019**, *143*, 433-440.
41. Braun, A. R.; Lacy, M. M.; Ducas, V. C.; Rhoades, E.; Sachs, J. N., alpha-Synuclein's Uniquely Long Amphipathic Helix Enhances its Membrane Binding and Remodeling Capacity. *J Membr Biol* **2017**, *250* (2), 183-193.
42. Vazdar, M.; Jurkiewicz, P.; Hof, M.; Jungwirth, P.; Cwiklik, L., Behavior of 4-hydroxynonenal in phospholipid membranes. *J Phys Chem B* **2012**, *116* (22), 6411-5.
43. Runfola, M.; De Simone, A.; Vendruscolo, M.; Dobson, C. M.; Fusco, G., The N-terminal Acetylation of alpha-Synuclein Changes the Affinity for Lipid Membranes but not the Structural Properties of the Bound State. *Sci Rep* **2020**, *10* (1), 204.
44. van Diggelen, F.; Hrlle, D.; Apetri, M.; Christiansen, G.; Rammes, G.; Tepper, A.; Otzen, D. E., Two conformationally distinct alpha-synuclein oligomers share common epitopes and the ability to impair long-term potentiation. *Plos One* **2019**, *14* (3), e0213663.
45. Bae, E. J.; Ho, D. H.; Park, E.; Jung, J. W.; Cho, K.; Hong, J. H.; Lee, H. J.; Kim, K. P.; Lee, S. J., Lipid peroxidation product 4-hydroxy-2-nonenal promotes seeding-capable oligomer formation and cell-to-cell transfer of alpha-synuclein. *Antioxid Redox Signal* **2013**, *18* (7), 770-83.
46. Domert, J.; Sackmann, C.; Severinsson, E.; Agholme, L.; Bergstrom, J.; Ingelsson, M.; Hallbeck, M., Aggregated Alpha-Synuclein Transfer Efficiently between Cultured Human Neuron-Like Cells and Localize to Lysosomes. *Plos One* **2016**, *11* (12), e0168700.

Appendices

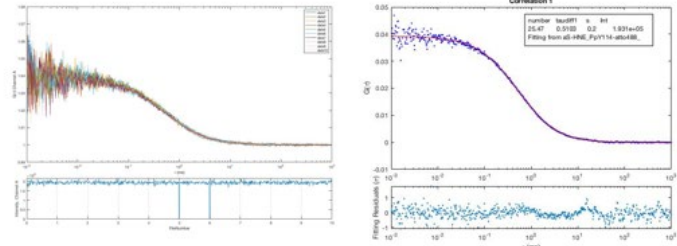
Appendix 1. SDS-PAGE gel of incorporated α S in aggregated samples of α S WT and α S-H50-HNE.



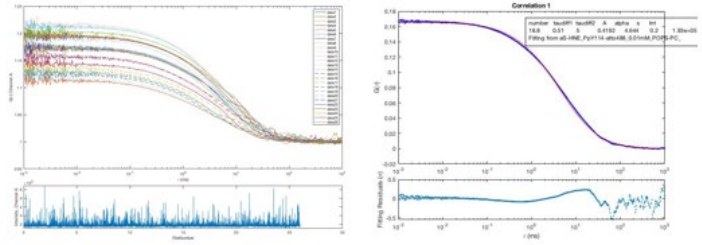
Appendix 2. Autocorrelation curves for α S-H50-HNE samples in buffer, 0.01 mM POPS/PC, and 0.01 mM POPS/PC.

Representative autocorrelation curves:

aS-HNE in buffer:



aS-HNE in 0.01 mM POPS/PC:



aS-HNE in 0.1 mM POPS/PC:

